REPUBLIC OF TÜRKİYE

YILDIZ TECHNICAL UNIVERSITY

GRADUATE SCHOOL OF SCIENCE AND ENGINEERING

DIELECTRIC AND THERMODYNAMIC PROPERTIES OF SMC* LIQUID CRYSTALS

Ihab Salah Mahdi AL-HUSAYNAT

Master of Science in Physics

Department of Physics

Physics Program

Supervisor

Prof. Dr. Nimet YILMAZ CANLI

February, 2024

REPUBLIC OF TÜRKİYE

YILDIZ TECHNICAL UNIVERSITY

GRADUATE SCHOOL OF SCIENCE AND ENGINEERING

DIELECTRIC AND THERMODYNAMIC PROPERTIES OF SMC* LIQUID CRYSTALS

A thesis submitted by IHAB SALAH MAHDI AL-HUSAYNAT in partial fulfillment of the requirements for the degree of MASTER OF SCIENCE is approved by the committee on 23.02. 2024 in Department of Physics, Physics Program.

Prof. Dr. Nimet YILMAZ CANLI
Yıldız Technical University
Supervisor

Approved By the Examining Committee

Prof. Dr. Nimet YILMAZ CANLI, Supervisor
Yildiz Technical University _____

Prof. Dr. Serap GÜNEŞ, Member
Yildiz Technical University _____

Prof. Dr. Ayşe ÇELİK BEDELOĞLU, Member
Bursa Technical University _____

I hereby declare that I have obtained the required legal permissions during data collection and exploitation procedures, that I have made the in-text citations and cited the references properly, that I haven't falsified and/or fabricated research data and results of the study and that I have abided by the principles of the scientific research and ethics during my Thesis Study under the title of **" DIELECTRIC AND THERMODYNAMIC PROPERTIES OF SMC* LIQUID CRYSTALS"** supervised by my supervisor, Prof. Dr. Nimet YILMAZ CANLI. In the case of a discovery of false statement, I am to acknowledge any legal consequence.

IHAB SALAH MAHDI AL-HUSAYNAT

Signature

Dedicated to my family

and my best friend

ACKNOWLEDGEMENTS

In closing this thesis, I thank everyone who contributed to its realization and rendered it an indelible experience.

Before anything else, I extend my most profound appreciation to my advisor, Professor Dr. Nimet Yilmaz Canli, for her unwavering support and guidance throughout the completion of this dissertation. I am indebted to her for the methodical instruction and tremendous effort that went into my scientific education.

Mr. Haider Mahmood AL Jaafer, I thank him for his invaluable support in bringing this thesis to fruition.

I want to extend my heartfelt appreciation to my spouse and children for their unwavering support and provision of all necessary for my academic achievements.

In conclusion, I sincerely appreciate my cherished parents and siblings for their unwavering support and affection.

IHAB SALAH MAHDI AL-HUSAYNAT

TABLE OF CONTENTS

ACKNOWLEDGEMENTS iv
TABLE OF CONTENTS v
LIST OF SAMPLE vii
LIST OF FIGURES viii
ABSTRACT x
ÖZET xii
1 INTRODUCTION 1
1.1 Literature Review 1
1.2 Purpose of the thesis 3
1.3 Hypothesis 3
2 LIQUID CRYSTALS 4
2.1 Brief History of Liquid Crystal 4
2.2 General Information 5
2.3 The categorization of liquid crystals 7
2.3.1 Thermotropic LCs 7
2.3.2 Lyotropic Liquid Crystals 8
2.4 Molecular Geometry of Liquid Crystals 8
2.4.1 Calamitic liquid Crystals 9
2.4.2 Discotic LCs 12
2.5 Chiral LCs 13
2.6 Phase Transitions in LCs 14
2.6.1 Classification of Phase Transitions 15
2.6.2 SmC*-I Phase Transition: 17
2.6.3 Cr-SmC* Phase Transition: 18
2.6.4 Landau-de Gennes Theory 19
2.6.5 Gibbs Free Energy 20
3 DIELECTRIC SPECTROSCOPY 22
3.1 Dielectrics 22
3.2 Dielectric Properties 23
3.3 Polarization 24
3.4 Dielectric Constant and Permeability 25
3.5 Connected Loads and Electric Displacement 26

3.6 Fundamental Equations in Dielectric Theory 29
3.7 Dielectric Relaxation and Cole–Cole Curves 31
3.8 Cole–Cole Equation 32
3.9 Temperature-Related Measurements and Activation Energy 33
4 MATERIAL AND METHOD **35**
4.1 Materials 35
4.2 Preparation of LC Cells 36
4.3 Devices and Equipment Used 37
5 RESULT AND DISCUSSION **41**
5.1 Mesomorphic Properties of LC1 and LC2 41
5.2. Dielectric Parameters of 5CB, 5CB+ 1%LC1 and 5CB+ 1% LC2 43
5.2. AC Conductivity of the Liquid Crystal Composites (5CB, 5CB+ 1% LC1 and 5CB+ 1% LC2)……..……47
5.3 Dielectric Parameters of LC1 Liquid Crystal at various temperatures 49
5.3. AC Conductivity of the LC1 at Various Temperatures 52
6 CONCLUSIONS **54**
REFERENCES **55**

LIST OF SAMPLE

ω	Angular Frequency
P_b	Connected Load Density
ε^*	Complex Dielectric Coefficient
ε_∞	Dielectric Coefficient at High Frequencies
ε_s	Dielectric Coefficient at Low Frequencies
μ	Dipole Moment
ε_0	Dielectric Permittivity of the Blank
D	Electric Displacement
E	Electric Field Vector
χ_e	Electrical Susceptibility
V	Electric Potential
P_f	Free Charge Density
F	Force Vector
ε''	Imaginary Part of the Complex Dielectric Coefficient
μ_0	Magnetic Permeability of Space
α	Polarizability
P	Polarization Vector
ε'	Real Part of the Complex Dielectric Coefficient
ε_r	Relative Permeability
τ	Stop Time
$\boldsymbol{\tau}$	Torque Vector (Electric Field Sourced)
W	Work

LIST OF FIGURES

Fig 2.1 The molecular configuration in the solid, liquid crystal, and liquid phases……..…..6

Fig 2.2 The categorization of typical liquid crystals……..…….…7

Fig 2.3 Molecular configurations within the Nematic LC…….….10

Fig 2.4 Molecular configurations within the Nematic LC……..11

Fig 2.5 Molecular configurations within the Smectic C phase……...12

Fig 2.6 (a) Nematic discotic and (b) Columnar discotic……..13

Fig 2.7 Molcules structure of cholesteric LCs…….……...14

Fig 2.8 An illustrative instance of phase transitions in relation to different macroscopic quantities: The diagram illustrates the schematic depiction of first-order phase transitions (a) and second-order phase transitions (b)……... 17

Fig 3.1 Calculating the polarisation of a dielectric substance and its corresponding surface area……..…….....27

Fig 3.2 Spherical body with shell permeability "2" and core permeability "1" in a permeability medium "3"……..…….....30

Fig 4.1 Chemical structure of 4-Cyano-4'-pentylbiphenyl (5CB)…….. 35

Fig 4.2 The molecule structure of LC1……..36

Fig 4.3 The molecule structure of LC2…….36

Fig 4.4 Empty cells (indium-tin-oxide (ITO) coated glass plates)……...36

Fig 4.5 Schematic representation of injecting the sample into the cell…….....37

Fig 4.6 Schematic representation of Impedance Analyzer…….....37

Fig 4.7 Schematic representation of temperature Controllers device……..38

Fig 4.8 Schematic representation of Kofler bank device…….38

Fig 4.9 Schematic representation of cryostats device……..….39

Fig 5.1 The Chemical structures of the (a) 5CB, (b) LC1 and (c) LC2……....41

Fig 5.2 DSC thermograms of compound LC1 on 2nd heating and cooling (10 °C min−1)…… ……..……...…… 42

Fig 5.3 DSC thermograms of compound LC2 on 2nd heating and cooling (10 °C min−1)…… ……..……...43

Fig 5.4 The real component of the dielectric constant versus angular frequency for (a) 5CB (b) 5CB+1% LC1 (C) 5CB+1% LC2 (d) comparative results…44

Fig 5.5 The results for imaginary components of the dielectric constant (a) 5CB (b) 5CB+1%LC1 (C) 5CB+1%LC2 (d) comparative results……....45

Fig 5.6 The Cole – Cole plots of (a) 5CB (b) 5CB+1%LC1 (C) 5CB+1%LC2 (d) comparative results……..46

Fig 5.7 The variation of ln σAC with angular frequency for (a) 5CB (b) 5CB+1%LC1 (c) 5CB+1%LC2 (d) comparative results…….....….48

Fig 5.8 The real component depend on angular frequency of LC1 at different temperatures (28 – 92 ºC)…… …….....49

Fig 5.9 The imaginary component depend on angular frequency of LC1 at different temperatures (28 – 92 ºC)……...……. 50

Fig 5.10 This chart show us the Cole – Cole curve of LC1 at different temperatures (28 – 92 ºC)…… …….51

Fig 5.11 ln σAC versus lnω graphics of LC1 at different temperatures…….....52

Fig 5.12 The Temperature dependence of lnσAC versus 1000/T of LC1 for ω=628 rad/s, ω=1253.025 rad/s and ω=4197.02 rad/s…….....53

ABSTRACT

DIELECTRIC AND THERMODYNAMIC PROPERTIES OF SMC* LIQUID CRYSTALS

IHAB SALAH MAHDI AL-HUSAYNAT

Master of Science in Physics

Department of Physics

English Program

Supervisor

Prof. Dr. Nimet YILMAZ CANLI

The chiral smectic liquid crystals (**LC1** and **LC2)** , namely (S) – 4 - n-octyl oxybenzylidene - 4' - (3,7-dimethyloctyloxy) aniline and (S) – 5 – n –octyloxy – 2 - [[[4 ' (3,7dimethyloctyloxy) phenyl] imino] methyl] phenol , are used as additives in the nematic liquid crystal **5CB** , which is composed of 4-cyano-4'-pentylbiphenyl. A comparison was made between the dielectric characteristics of **5CB** doped with 1wt.% chiral smectic liquid crystals (**LC1**, **LC2**) and pure **5CB**. We employed the dielectric spectroscopy technique to ascertain the dielectric characteristics of the 1wt.% concentration of liquid crystals doped with **5CB** liquid crystal. The capacitance approach has determined the dielectric constant's actual (ε′) and imaginary (ε″) parts. The parameters of the all-dielectric have been computed and compared. The results of polarized microscopy indicate that **LC1** and **LC2** have an enantiotropic chiral smectic mesophase. The SmC* phase transition in the chiral liquid crystal has been extensively studied. Typically, the SmC*-I exhibits first-order behavior. Dielectric spectroscopy and differential

scanning calorimetric (DSC) studies were employed to investigate phase transitions. Dielectric measurement is a highly effective technique for determining phase sequence and investigating phase transition. The analysis of phase transitions, dielectric characteristics of **LC1** was conducted using impedance spectroscopy measurement throughout a range of temperatures spanning from 28 to 92 degrees Celsius.

Keywords: Phase transition temperatures, Differential scanning calorimetry (DSC), thermodynamic, Liquid crystal, Dielectric properties

ÖZET

SmC* Sıvı Kristallerin Dielektrik ve Termodinamik Özellikleri

IHAB SALAH MAHDI AL-HUSAYNAT

İngilizce Programı

Yüksek Lisan Tezi

Danışman

Prof. Dr. Nimet YILMAZ CANLI

Kiral smektik sıvı kristaller **LC1** ((S) – 4 - n-oktiloksibenziliden - 4 ' -(3,7-dimetiloktiloksi) anilin) ve **LC2** (S) – 5 -n-oktiloksi – 2 - [[[4' - (3) ,7-dimetiloktiloksi) fenil] imino] metil]fenol , nematik sıvı kristal 5**CB**'ye (4 – siyano - 4' – pentilbifenil) katkı yapmak için kullanıldı. Ağırlıkça %1 kiral smektik sıvı kristaller (**LC1**, **LC2**) ve saf **5CB** ile katkılı **5CB**'nin dielektrik özellikleri karşılaştırıldı. **5CB** sıvı kristaline ağırlıkça %1 katkılı LC'lerin dielektrik özelliklerini belirlemek için dielektrik spektroskopi yöntemini kullandık. Dielektrik sabitinin gerçek (ε ′) ve sanal bileşenleri (ε ″) kapasitans yöntemiyle hesaplanmıştır. Tüm dielektrik parametreler hesaplandı ve karşılaştırıldı.

Polarize edici mikroskopi sonuçları, **LC1** ve **LC2**'nin enansiyotropik kiral smektik mezofaz sergilediğini göstermektedir. Kiral sıvı kristalde SmC* faz geçişi yoğun araştırmaların konusu olmuştur. Çoğu durumda SmC*-I birinci derecedendir. Faz geçişleri, dielektrik spektroskobisi ve diferansiyel taramalı kalorimetrik (DSC) analizi ile incelenmiştir. Dielektrik ölçümün kullanılması, faz sırasını belirlemek ve faz geçişini araştırmak için de iyi bir yöntemdir. **LC1**'in faz geçişleri, dielektrik özellikleri ve ac

iletkenlik mekanizması farklı sıcaklıklarda (28-92 ºC) empedans spektroskopisi ölçümü ile analiz edilmiştir.

Anahtar Kelimeler: Faz geçiş sıcaklıkları, Diferansiyel taramalı kalorimetri (DSC), Termodinamik, Sıvı kristal, Dielektrik özellikler

1
INTRODUCTION

1.1 Literature Review

Liquid crystals are a distinct form of matter characterized by a liquid-like flow and crystal-like molecular alignment with directional properties. These intriguing materials have attracted considerable attention in several fields because of their exceptional features and extensive range of uses. This literature review aims to present a thorough and detailed examination of liquid crystals, with a specific emphasis on their structural features, categorization, physical attributes, and utilization in several domains [1].

The classification of liquid crystals is predicated upon two primary classifications: thermotropic and lyotropic. Thermotropic liquid crystals (LCs) experience changes in their physical state as the temperature varies. In contrast, lyotropic LCs are formed by the self-organization of molecules with both hydrophilic and hydrophobic properties in solvents [2]. Thermotropic liquid crystals can be classified into several phases, namely nematic, smectic, cholesteric, and discotic, depending on the arrangement of their molecules.

The arrangement of component molecules substantially influences the behavior of liquid crystals, particularly concerning molecular structure and phase transitions. Typical LC molecules exhibit various morphologies such as elongated, flat, and round.

Phase transitions between distinct liquid crystal (LC) phases transpire due to alterations in temperature, pressure, or external fields. Comprehending these changes is essential for advancing LC-based technologies and materials [3].

Liquid crystals provide intriguing optical characteristics, these materials, which exhibit birefringence and polarisation effects, are very suitable for applications such as screens, modulators, and optical switches their unique electrical properties, such as dielectric anisotropy, have led to the development of liquid crystal displays (LCDs) and adjustable devices. Furthermore, LCs have viscoelastic properties that affect the features of their flow, making them highly important in technologies that are based on liquid crystal (LC)

materials [4].

LCDs (liquid crystal displays) include significantly transformed the display industry and are currently ubiquitous in electronic devices. Encompassing computer displays, mobile phones, and televisions. The fundamental components of LCDs consist comprising polarizers, a liquid crystal layer, and an illumination situated between glass substrates. Developments in organic light-emitting diodes (OLEDs) and in-plane switching (IPS) have propelled LCD technology forward, has enhanced the accuracy of color reproduction, widened the range of viewing angles, and increased energy efficiency.

Numerous optoelectronic and photonic apparatus rely heavily on liquid crystals. Real-time light management is made possible by LC adjustable lenses and beam steerers, which facilitate adaptive optics and efficient beam manipulation. Photonic crystals in liquid form and metamaterials possess distinctive optical characteristics, which have the potential for the development of innovative technologies such as slow light devices and optical sensors.

Liquid crystals have evolved into highly important in sensor technology because of their responsiveness to external stimuli, such as temperature, pressure, and chemical composition. Liquid crystal (LC) biosensors are now under development for healthcare and biological purposes, providing the ability to detect biomolecules in real-time without labels. Furthermore, these sensors have potential in environmental monitoring and food safety [5].

The latest research on liquid crystals has revealed promising prospects for forthcoming applications. Utilizing liquid crystals and flexible and wearable electronics provides novel design possibilities and improved user satisfaction. Liquid crystal-based artificial intelligence and neuromorphic computing investigate non-traditional approaches to computing. Incorporating liquid crystals into soft robotics and stretchy electronics allows for creating versatile and flexible systems with several functions [6]. Liquid crystals remain intriguing to academics and engineers due to their adaptable characteristics and extensive range of applications. Liquid crystals have significantly influenced several sectors, ranging from displays and sensors to optoelectronics and medicine. With the progression of technology and our enhanced comprehension of liquid crystals, we may expect a proliferation of inventive applications and revolutionary products [7]. This comprehensive introduction delves into the historical history, many uses, and

groundbreaking impact of liquid crystals on modern technology. The intricate correlation between research and innovation, which persistently impacts our technological milieu, will become increasingly evident as our understanding of the properties and applications of liquid crystals deepens.

1.2 Purpose of the thesis

"**Dielectric and Thermodynamic Properties of SmC* Liquid Crystals"** This term relates to a scientific research effort that examines and assesses the dielectric properties of chiral liquid crystals which undergo phase transitions. Dielectric characteristics pertain pertaining to the response of substances to an electric field. Within the scope of the examination, the primary objective is to examine the behavior of various liquid crystals when subjected to electric fields during phase transitions and to analyze the alterations in their dielectric properties at varying temperatures. Thermodynamics is the study of the interplay between heat and other types of energy inside a system. This study focuses on analyzing the thermodynamic characteristics of liquid crystals, explicitly investigating their enthalpy variations and heat transfer mechanisms that occur during phase transitions. This research aims to further our comprehension with regard to dielectric behaviour and properties of liquid crystals that demonstrate phase transition temperatures. The discovery has significant implications in several industries, including display technologies, sensors, and other electronic devices that necessitate materials with precise thermal and dielectric characteristics.

1.3 Hypothesis

Liquid crystals are substances that exhibit dielectric properties. The dielectric spectroscopy method is a convenient approach for correctly analyzing these properties. The primary objective of dielectric research has been to establish a correlation between the dielectric constant and the molecular characteristics of liquid crystals.

We planned to adding liquid crystals at 1% concentrations to commercial liquid crystal **5CB** at room temperature. It was expected that improvements in the properties of dielectric. We also tried to find the phase transition temperatures from sudden changes in dielectric properties depending on temperature.

2
LIQUID CRYSTALS

2.1 Brief History of Liquid Crystal

The history of liquid crystals spans over a century and is characterized by a captivating journey of exploration and advancement. Austrian botanist Friedrich Reinitzer discovered liquid crystalline characteristics while investigating cholesterol benzoate in the late 19th century. This serendipitous finding served as the initial insight into the distinctive characteristics of liquid crystals [8].

Over the following decades, researchers persisted in examining these captivating chemicals. Nevertheless, it was only in the 20th century that their importance became increasingly evident. X-ray diffraction research acquired significant knowledge regarding the organized molecular structures present in liquid crystalline phases, providing valuable insights.

Physicist Sir Charles Frank coined the phrase "liquid crystal" during the 1950s. His groundbreaking research and Additional researchers advanced the comprehension of liquid crystals, characterizing them as an intermediary phase between solids and liquids. This categorization established the basis for subsequent investigation of their distinct characteristics [9].

Liquid crystals made their initial practical debut in the 1960s by creating liquid crystal displays (LCDs). George H. Heilmeier and Wolfgang Helfrich developed the inaugural LCDs. Information presentation was made possible by these displays by using electrical fields to manipulate the alignment of liquid crystal molecules. This milestone marked the beginning of modern flat-panel display technology.

During the 1970s and 1980s, LCDs were prevalent in tiny electronic devices such as calculators and digital watches, primarily because of their low power consumption and compact size. Nevertheless, it was not until the 1990s when LCDs experienced significant growth, becoming widely used in computer monitors, TVs, and other display applications. Due to its adaptability and advances, liquid crystal technology quickly supplanted other display technologies, such as cathode ray tubes (CRTs).

Liquid crystal displays have emerged as the prevailing technology in the display industry over the 21st century, fundamentally transforming our interaction utilising electronic devices. Multiple LCD technologies, including twisted nematic (TN), in-plane switching (IPS), and organic light-emitting diodes (OLEDs), have undergone significant development, has significantly enhanced the quality and efficiency of displays [10].

Currently, liquid crystals constitute a fundamental component of contemporary society, present in smartphones, tablets, computers, televisions, and several other electronic gadgets. The current investigation into liquid crystals produces encouraging outcomes, investigating novel applications and pioneering technologies in domains such as sensors, optical devices, and even biological research [11].

As we explore further into the captivating realm of liquid crystals, their capacity for future advancements remains limitless. Researchers and technologists persist in investigating and using the distinct characteristics of these substances, driving us towards a future abundant with more remarkable uses and progressions [12].

2.2 General Information

LC is a distinct phase of matter that displays properties consisting of liquids and crystals It serves as a transitional state between the chaoticThe liquid exhibits a structure that resembles that of a fluid. Meticulously organised molecular arrangement of a solid crystal. In LC, the molecules exhibit a degree of alignment and positional arrangement, resembling that of a crystal. Nevertheless, they possess Fluidity and exhibit fluid-like movement [8].

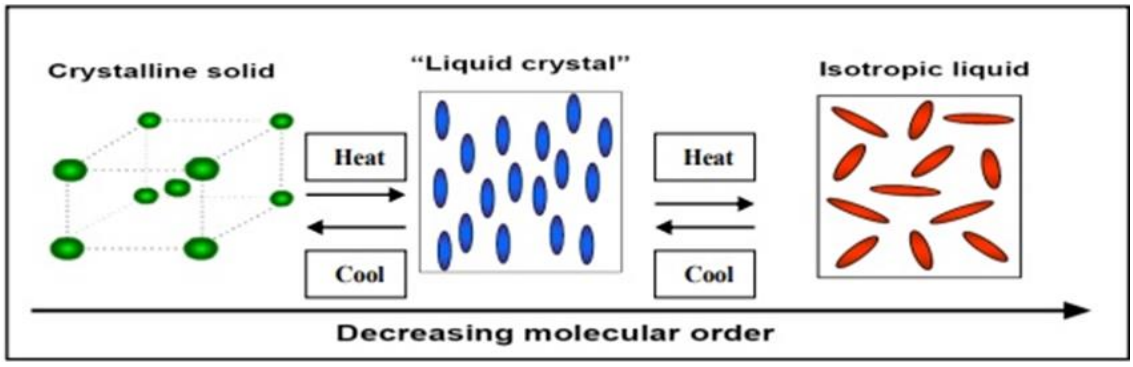


Fig 2.1 The molecular configuration in the solid, liquid crystal, and liquid phases**.**

The distinctive properties exhibited for LCs stem due to the anisotropic nature of their molecular structure. Anisotropy refers to the phenomenon where the characteristics of a material exhibit variation depending on the direction in which they are measured. Within ın a liquid crystal, the molecules have a tendency to align themselves along a certain axis called the director. This alignment remains continuous across short distances, resulting in the creation of localised order within the material [13].

LCs are able to go through phase transitions in response to variations Regarding temperature, pressure, or any other environmental stimuli. The predominant phase transition in liquid crystals is the shift from the nematic phase, characterized by aligned molecules that retain freedom of movement, to the isotropic phase, when molecular alignment is lost, and the material exhibits normal liquid behavior.

The remarkable characteristics of liquid crystals have resulted in several practical implementations, notably in display technology. LCDs use the capacity of liquid crystal molecules to orient themselves in reaction to electric fields, therefore regulating the transmission of light and facilitating the presentation of pictures and data. Liquid crystal displays (LCDs) are widely employed in many electronic devices, including televisions, computer monitors, cell phones, and tablets [14].

Liquid crystals have many uses in sectors such as optoelectronics, photonics, sensors, and biological research, in addition to its use in display technologies. Due to their adjustable optical and electrical characteristics, they possess significant value in several contemporary technologies. The ongoing exploration and comprehension of liquid crystals by researchers is expected to considerably enhance their potential for novel applications.

2.3 The categorization of liquid crystals

Two primary classifications of liquid crystals can be established according to their reactivity to variations in temperature or concentration [15]:

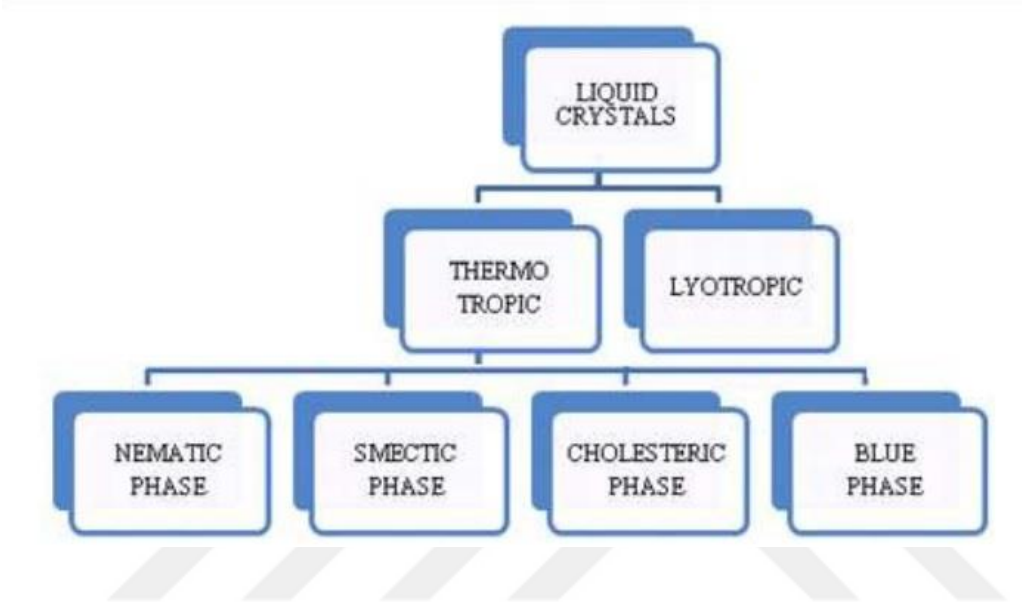


Fig 2.2 The categorization of typical liquid crystals [16]**.**

2.3.1 Thermotropic LCs

Phase transitions occur in thermotropic liquid crystals in response to changes regarding temperature. These transitions take place within certain temperature ranges. Causing the liquid crystal to transform from one ordered phase to another. The primary phases that comprise thermotropic LCs are [17]:

(A) The nematic Phase: Molecules align in a preferred direction during this phase, but they are free to rotate and move about their long axis.

(B) The smectic Phase: Smectic phase molecules are arranged in layers according to their long-range positional order within each layer. A layer is composed of molecules that have a predetermined orientation.

(C) Frequently referred to as the chiral nematic phase, this particular state is distinguished by its helical configuration of molecules that are contorted.

(D) The smectic C Phase: which is A subdivision of the smectic phase. Has a molecular arrangement that is inclined relative to the layer normal.

(E) The smectic A Phase an additional subclass of the smectic phase is known as the smectic A the molecular arrangement of a phase is inclined, but the tilt is consistent throughout the layers.

(F) Smectic B Phase: The smectic B phase molecules exhibit a disordered orientation and a tilted position within the layers [18].

2.3.2 Lyotropic Liquid Crystals

By means of the self-assembly of amphiphilic molecules in solvents, typically water, lyotropic liquid crystals are generated. In lyotropic liquid crystals, phase transitions transpire in response to variations in concentration as opposed to temperature. The following are the primary phases of lyotropic liquid crystals [19]:

(A) The Lamellar Phase: Analogous to the smectic phase observed in thermotropic liquid crystals, the molecules exhibit long-range positional order as they form layered layers during this phase.

(B) Hexagonal Phase: Within the strata, the molecules are organised in a hexagonal lattice structure.

(C) Micellar Phase: Spherical micelles, formed by the aggregation of molecules, are dispersed throughout the solvent.

This system of classification aids scientists and researchers in comprehending the behaviour of various liquid crystal varieties under particular conditions. Exploring the unique properties and potential applications of thermotropic and lyotropic liquid crystals is facilitated by the distinction between the two. Such applications include display technology, optics, sensors, and more [20].

2.4 Molecular Geometry of Liquid Crystals

In liquid crystals, the molecular geometry pertains to the configuration and orientation of the individual molecules that comprise the liquid crystal phase. The study of geometry is essential in establishing the macroscopic characteristics and behavior of liquid crystals.

Liquid crystals commonly contain molecules that exhibit an elongated or rod-like morphology, although alternative configurations, such as disc-like or plate-like molecules, are also possible. The distinctive characteristics of these molecules are due to the anisotropic nature of their interactions along distinct axes [21].

Nematic liquid crystals exhibit molecular alignment along a common axis, referred to as the "director," while preserving their inherent mobility and rotational capabilities. In this phase, the arrangement of molecules produces an orientational order over extended distances but no positional order [22].

During smectic phases, the molecules arrange themselves in strata according to long-range positional order within each layer. An inclined molecular arrangement can result from the varying orientations of the molecules within a layer, as observed in the smectic C and smectic A phases.

The chiral nematic phase also called the cholesteric phase, demonstrates a molecular arrangement characterized by a helical rotation of the director within the substance. The distinctive colors observed in cholesteric liquid crystals under specific conditions are due to the helical structure [23].

It is essential to comprehend the molecular geometry of liquid crystals to determine how they react to external stimuli like pressure, temperature, and electric fields. It affects liquid crystals' phase transitions and optical, electrical, and mechanical properties. Utilizing this molecular geometry, scientists and engineers engineer and design liquid crystal materials with particularization in mind, catering to applications including liquid crystal displays (LCDs), sensors, and various optoelectronic devices [24].

2.4.1 Calamitic liquid Crystals

Calamitic liquid crystals, which are alternatively named rod-shaped, are classified as liquid crystals due to their molecular structure resembling a rod. "Calamitic" is derived from the Greek word "kalamos," which translates to "reed" or "rod." These molecules generally have an elongated axis and demonstrate anisotropic properties, indicating that their physical attributes differ according to the direction [25].

The most prevalent form of liquid crystals, calamite liquid crystals, is utilized as the building blocks for various liquid crystal technologies, including liquid crystal displays (LCDs). The rod-like morphology of these entities induces them to align in a common

direction when exposed to external forces or electromagnetic fields. As a result of this alignment, liquid crystals exhibit many ordered phases, including nematic, smectic, and cholesteric phases [26].

One of the most notable phases is the nematic phase, characterized by molecules aligned parallel to each other but lacking any discernible order of position. In contrast, subphases such as Smectic A (SmA) and Smectic C (SmC) result from the formation of positionally ordered layers within the molecules during the smectic phases [27].

The nature of these subphases is determined by the molecular axes' orientation relative to the layer's normal.

Calamitic liquid crystals are paramount in contemporary display technologies due to their remarkable ability to alter their optical properties in response to electric fields. By aligning these rod-shaped molecules in response to an electric field, light transmission can be precisely regulated, facilitating the generation of images and data on LCDs.

Calamitic liquid crystals represent an essential and extensively studied class of materials that find utility in many contexts, rendering them essential constituents in numerous modern technologies [28].

Nematic liquid crystal

Nematic LCs are a specific category of liquid crystals that are notable for their distinctive molecular alignment and characteristics. The name "nematic" originates from the Greek word "nema," which signifies "thread," alluding to the thread-like organisation of molecules found in this phase [29].

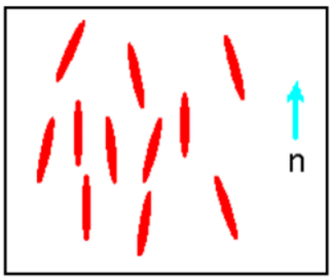


Fig 2.3 Molecular configurations within the Nematic LC.

During the nematic phase, the liquid crystal's molecules are in a parallel alignment, reminiscent of the strands in a fabric. In contrast to solid crystals, molecules in the nematic phase are mobile and capable of rotation about their long axis, similar to the behavior observed in liquid states. Although the molecules prefer a common direction of alignment, this configuration produces an ordered state with no fixed positional order. [30].

Nematic liquid crystals have anisotropic properties, which indicate that their physical characteristics vary by the direction of the molecular alignment. Distinctive optical properties result from the varying refractive indices exhibited along and perpendicular to the alignment vector. Furthermore, in response to an external electric or magnetic field, nematic liquid crystals align the direction of the field [31].

The capacity of nematic liquid crystals to alter their configuration in reaction to external stimuli holds excellent importance within liquid crystal display (LCD) technology. LCDs can regulate light transmission and produce visually appealing images or informational displays by using electric fields to manipulate molecular alignment.

Nematic liquid crystals find wide-ranging utility in fields such as optics, photonics, sensors, and liquid crystal lenses, in addition to display technology. Continuous research is devoted to developing novel nematic liquid crystal materials with particular properties, thereby expanding their application in various contemporary technologies [32].

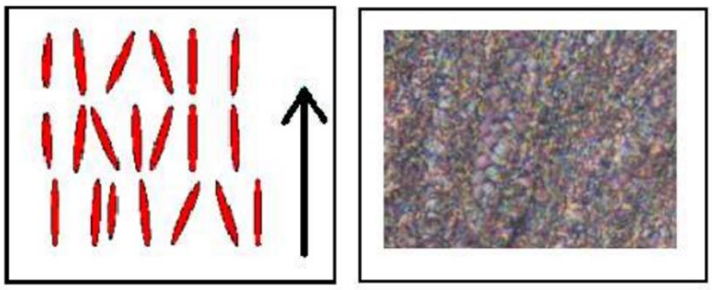


Fig 2.4 Molecular configurations within the Nematic LC**.**

Smectic liquid crystal

The smectic phases, which generally transpire at reduced temperatures compared to the nematic phase, witness the layering of liquid crystal molecules [33]. This causes each stratum to be arranged in a unidirectional positional order [34]. Smectic phases come in a variety of varieties, including Smectic A (SmA), Smectic C (SmC), Smectic B (SmB), Smectic F (SmF), Smectic I (SmI), and Smectic E (SmE), which are higher order. The

molecules, on average, align in the Smectic A phase along the normal of the layer. However, in the Smectic C phase, the average molecular direction becomes angular to the normal of the layer [35].



Fig 2.5 Molecular configurations within the Smectic C phase.

2.4.2 Discotic LCs

Discotic LCs, often referred to as columnar phases, are formed by molecules having a disc-like structure, commonly known as "discotic mesogens." These materials generally have a central aromatic nucleus around flexible aliphatic chains. These mesogenic compounds consist of a disk-shaped aromatic core surrounded by flexible aliphatic groups [36].

The arrangement of discotic molecules during nematic discotic mesophase is strikingly similar to the alignment observed in calamitic mesogen nematic mesophases. The strata of disc-shaped molecules in the Nematic Discotic Mesophase display an almost parallel orientation [37].

The columnar discotic mesophase results from the self-assembly of disc-shaped molecules into columns, driven by intermolecular interactions. The Columnar Mesophase can be categorised based on the two-dimensional lattice symmetry inside the column as either hexagonal, right-angled rectangle, or oblique angle.

Furthermore, it can be categorized as regular or irregular according to the stacking pattern inside the fundamental cell [38].

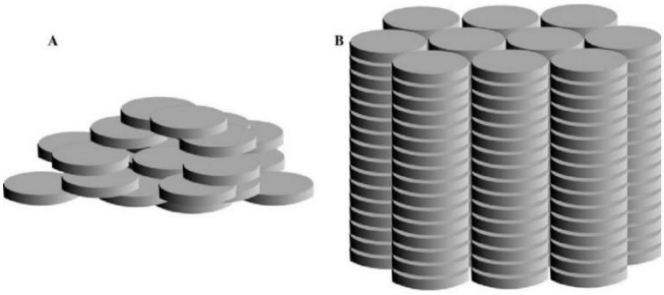


Fig 2.6 (a) Nematic discotic and (b) Columnar discotic [39]**.**

2.5 Chiral LCs

Chiral liquid crystals, also known as chiral nematic or cholesteric liquid crystals, represent a unique category of liquid crystal substances distinguished by their chiral (twisted) molecular structure. The molecular configuration of these substances is helical or spiral, in contrast to the linear or parallel arrangement commonly observed in nematic liquid crystals [40].

Chiral refers to the property of chirality, which means that the molecular structure cannot be superimposed onto its mirror image, similar to the difference between the left and right hands [41].

Numerous distinctive optical properties result from the existence of this chiral configuration, including the preferential reflection of circularly polarised light; this results in the generation of vivid and scintillating colors. Chiral liquid crystals are utilized in various display and optical technologies, such as reflective color displays, optical filters, and cholesteric displays [42].

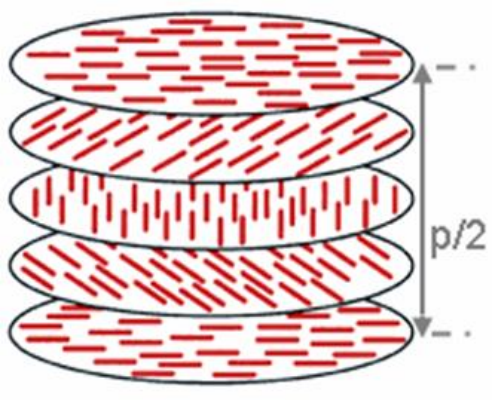


Fig 2.7 Moleculer structure of cholesteric LCs.

2.6 Phase Transitions in LCs

It involves alterations in the molecular structure and arrangement inside a material made up of liquid crystals. These alterations are prompted by variations in temperature, pressure, or other external stimuli. Liquid crystals are a distinct state of matter that exhibits properties of both liquids and crystalline solids. These materials can experience phase transitions due to changes in the external environment.. The positional and orientational arrangement of liquid crystals allows them to be categorized into five distinct phases [43]. The following phases are included in this sequence: Liquid, nematic, smectic, columnar, and crystalline compounds comprise the phases. A significant level of molecular organization characterizes crystals, as molecules are confined to particular positions and are arranged in them. Particles in liquids demonstrate random motion in every direction. Liquid crystal is an intermediate state that lies between two other states, and its classification is based on varying levels of organization [44]. The nematic phase represents the highest level of chaos. The substance displays orientational order, known as a director, but does not possess positional order. During the smetic phase, molecules are organized in sheets that have a clearly defined space between them and a certain orientation. Conversely, in the columnar phase, molecules are arranged in a disk-like manner, forming columns that give rise to a two-dimensional array. Isotropic liquids undergo a sequential transition into the nematic, smectic, and columnar phases when they are cooled. Phase transition in liquid crystal is characterized by tiny cooperative contacts, as well as spontaneous symmetry breaking, substantial fluctuation, divergent susceptibility, and discontinuity [45].

2.6.1 Classification of Phase Transitions

First-order phase transitions in LCs : refer to abrupt and non-continuous alterations in the arrangement and orientation of LC molecules due to changes in external factors like temperature and pressure. These transitions entail a sudden shift from one phase to another, sometimes accompanied by the absorption or release of latent heat. The following are common instances of first-order phase transitions in liquid crystals (LCs) [46].

Transition from an isotropic phase to a nematic phase : During this phase transition, the state of severe disorder known as the isotropic phase undergoes a transformation into the state of partial order called the nematic phase. As the temperature falls, the alignment of molecules increases, while a certain level of chaos still remains.

Transform from Nematic to Smectic: A frequently observed first-order transition takes place between nematic and smectic phases, including SmA, SmB, and SmC. By means of this conversion, a partially organized nematic structure is converted into a stratified, structurally ordered smectic structure while the orientation of molecules is preserved.More precisely, the transition from one smectic phase to another (e.g., SmA to SmC) within liquid crystals (LCs) may manifest as a first-order transition. In the SmA phase, molecules exhibit alignment and organize themselves into distinct strata. Throughout the SmC phase, the molecules manifest an inclination in opposition to the normal of the layer, resulting in the formation of a chiral structure [47].

Transform from Cholesteric to Smectic: Some liquid crystals (LCs) exhibit a first-order transition from the cholesteric phase, which is characterized by a helical molecule structure, to the smectic phase. This often involves modifications in the pitch of the cholesteric helix.

First-order phase transitions in liquid crystals (LCs) occur at a predetermined temperature and are characterised by the sudden appearance or disappearance of specific structural features, such as layering or handedness. The transitions have a substantial effect on the physical and optical properties of LC materials, making them crucial for many applications such as liquid crystal displays (LCDs), optical devices, and sensors [48].

It is imperative to recognise that the particular attributes of first-order phase transitions may vary across liquid crystal materials characterised by distinct properties. Comprehending and controlling these initial changes in state is crucial for customizing liquid crystals for a wide range of technological uses [49].

Phase transitions of the second order in liquid crystals: In contrast to first-order phase transitions, which involve abrupt and continuous changes and the dissipation or absorption of latent heat, second-order phase transitions in liquid crystals (LCs) are distinguished by incremental modifications in the order parameter and the absence of latent heat. Variations in external factors such as pressure, temperature, or an applied field cause the progressive alteration of LCs' properties during second-order phase transitions. Multiple occurrences of second-order phase transitions are prevalent in liquid crystals [50].

Transform from Isotropic to Nematic : The transition from an isotropic phase to a nematic phase is typically classified as a first-order transition, although in certain liquid crystals, it may exhibit second-order properties. A progressive increase in alignment and a continuous decrease in molecular disorder are observed under these conditions as the temperature decreases. An enduring modification in the order parameter distinguishes the transition.

Similarly, the nematic-to-smectic transition : It might sporadically demonstrate second-order characteristics. As the liquid crystal is chilled, a progressive manifestation of translational order distinguishes the transition from a nematic, partially ordered state to a smectic, stratified arrangement.

The transformation from one clearly defined smectic phase to another (from SmA to SmC) It is generally of the second order. A continuous evolution occurs in the inclination of the molecule's orientation with respect to the normal of the layer throughout these transitions. As a consequence, the SmA structure undergoes a transformation into the SmC structure, which is distinguished by the existence of inclined molecules.

The transition between cholesteric and smectic phases Furthermore, it has the capability to exhibit second-order attributes. This transition usually involves adjustments to the pitch of the cholesteric helix. Second-order transitions are characterized by continuous variations in intonation. Second-order phase transitions involve a gradual and smooth change in physical properties as an external input, usually temperature, changes.

These transitions are generally linked to critical phenomena, and the order parameter, such as the pitch of a cholesteric helix or the degree of alignment, undergoes a gradual evolution devoid of sudden alterations. It is of the utmost importance to comprehend second-order phase transitions in liquid crystals (LCs) to tailor their properties to particular specifications, as in the case of liquid crystal displays (LCDs), optical devices, and sensors [51]. The specific attributes of these transitions may differ contingent upon the particular qualities possessed by the LC material under consideration.

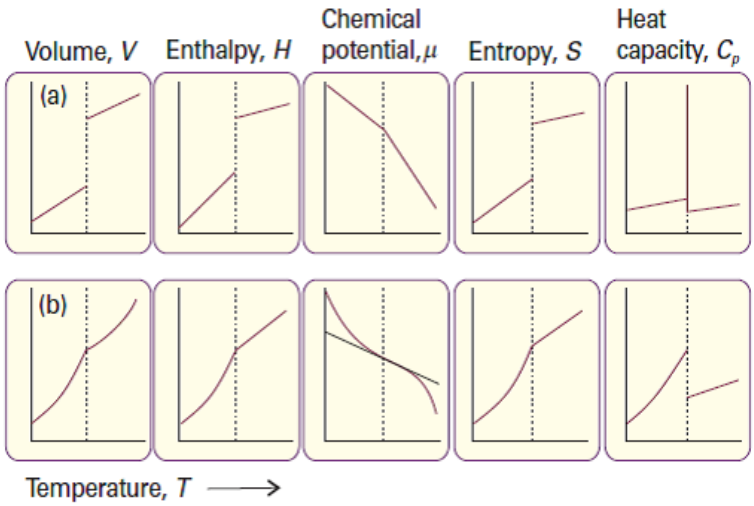


Fig 2.8 An illustrative instance of phase transitions in relation to different macroscopic quantities: The diagram illustrates the schematic depiction of first-order phase transitions (a) and second-order phase transitions (b) [52].

2.6.2 SmC*-I Phase Transition:

The SmC*-I Phase Transition: A ferroelectric SmC* phase transition occurs in the SmC phase, which is composed of molecules with electric dipole moments. The free energy model in this transition is expressed in terms of coupled order parameter terms including spontaneous polarization. The various phases that can arise are thoroughly examined, and the circumstances in which the change from an isotropic liquid to the SmC* phase takes place are looked at. Over the past 20 years, significant advancements have been made in the field of ferroelectric liquid crystal. Layered structures make up smectic phases. The layer normal k and the n-direction vector form an angle θ during the SmC phase. Layer by layer, the SmC* phase rotates. Along the smectic layers, spontaneous electric

polarization P_ρ is produced by this symmetry breakdown in nanoscale electric dipoles. Experiments have shown that the chiral smectic C-isotropic liquid (SmC*-I) phase transition has a first-order feature. The SmC*-I mesophase is first-order, as indicated by the sharp increase in enthalpy at the transition point. The spontaneous electrical polarization in the SmC* phase has a mild temperature dependency, the slope angle θ' has a finite value, and the spontaneous polarization of the SmC*-I transition has a finite value, according to electro-optical observations in chiral derivatives. The SmC*-I transition's first-order character is further supported by sharp peaks in heat capacity measurements . Mukherjee has constructed a Landau model to explain the terms in the SmC*-I transition and the nature of this transition, as there is not much practical work available due to its intricacy. This method is comparable to the transitions between I-SmA and I-SmC. The free energy (F) for the SmC* phase is expressed as follows [53].

$$F=F_0^*+\frac{3}{4}DS+\frac{3}{4}A^{**}S^2-\frac{1}{4}B^{**}S^3+\frac{9}{16}C^{**}S^4 \qquad (2.1)$$

In the context of the equation, the B** cubic coefficient indicates, according to Mean-Field theory, that the I-SmC* phase transition must always be of first order.

2.6.3 Cr-SmC* Phase Transition:

The phase transition from chiral smectic C liquid crystal (SmC*) to crystalline (Cr) occurs during the Cr-SmC* phase transition. This signifies a modification in the molecular arrangement and order of the compound. The transition temperature (Cr-SmC*) is an essential parameter that specifies the particular circumstances, which are typically dependent on temperature, in which this phase transition takes place. The determination of the orientation of molecules within the smectic layers during the transition is heavily reliant on the angle theta (θ). The angle formed between the direction of molecular alignment (n-direction vector) and the layer normal (k) is denoted as theta during the SmC* phase. The insights into the structural changes and molecular reorganization that occur during the transition can be gleaned from the variation in theta. Molecular arrangement in the Cr phase is frequently more crystalline and ordered than in the liquid crystal phases. Diverse applications, including the creation of sophisticated materials,

liquid crystal displays (LCDs), and optical devices, may be affected by this transition. Gaining insight into the intricacies of the phase transition between Cr and SmC* enables scientists to manipulate and regulate the characteristics of liquid crystals, thereby facilitating technological progress and the development of innovative materials featuring customized functionalities [53].

2.6.4 Landau-de Gennes Theory

By utilizing this mathematical framework, the behavior of liquid crystals can be described. Free energy, phase transitions, and system parameters are the focal points of this theory. This facilitates understanding the responses of liquid crystals to changes in temperature, external fields, and spatial configuration. Furthermore, the influence of external fields and the characteristics of phase transitions are considered. Using numerical simulations, this theory is frequently implemented to forecast the behavior of liquid crystals. This material has practical uses and is used in fundamental research in several technologies, including liquid crystal grindings, liquid crystal optics, optical devices, and liquid crystal displays [54].

The Landau-de Gennes theory may be employed to clarify both first-order and second-order phase transitions in liquid crystals. The order parameter components of the Landau-de Gennes free energy functional are employed in distinct transition equations.

During a first-order phase transition, the free energy density (f(Q)) generally exhibits a double-well potential, wherein two minima correspond to coexisting phases. [55]. At the phase transition, the order parameter (Q) may experience an abrupt change due to a leap between these minima. The Landau-de Gennes free energy functional for a first-order transition is represented by the given expression.

$$F[Q]=\int_V \left(f(Q)+ k/2\ (\nabla Q)^2\right) dV \qquad (2.2)$$

The equation involves the free energy density, denoted as f(Q), which varies depending on the specific characteristics of the system. A first-order transition should have several minima, which indicate the presence of phases.

During a second-order phase transition, the free energy density (f(Q)) shows a single minimum, and the order parameter undergoes a continuous change as the system goes through the phase transition temperature or condition.Equation (2.2) is the Landau-de Gennes free energy functional for a second-order transition.The function f(Q) often possesses a single minimum and commonly displays a Landau expansion that encompasses terms up to the fourth order in the order parameter. The Landau-de Gennes theory distinguishes between first- and second-order transitions by analysing the shape of the free energy density (f(Q)) and the behaviour of the order parameter (Q) in response to variations in temperature or other relevant factors [56].

2.6.5 Gibbs Free Energy

The Gibbs free energy (G), denoted in thermodynamics, is a thermodynamic potential utilised to compute the maximum amount of work that a thermodynamically closed system can accomplish at a constant pressure and temperature, excluding pressure-volume work. Additionally, it is necessary for chemical reactions and other processes that may take place under these conditions [57]. The Gibbs free energy can be expressed as

$$G_{(P,T)} = U + PV - TS = H - TS \tag{2.3}$$

The symbols used in thermodynamics are as follows: V for volume, P for pressure, T for temperature, H for enthalpy, and S for entropy are represented by the letters U through S. The Gibbs free energy change ($\Delta G = \Delta H - T\Delta S$) represents the maximum non-volume expansion work that can be generated within a closed system operating at a constant pressure and temperature. A closed system can only exchange heat and work with its surroundings; it cannot exchange matter. Such attainment is exclusively possible via an utterly reversible procedure [58]. during a reversible transition from an initial state to a final state, the reduction in Gibbs' free energy is equivalent to the effort exerted by the system on its environment minus the effort exerted by the pressure forces. The Gibbs energy is the thermodynamic potential reduced to its minimum value when a system attains chemical equilibrium at room temperature and pressure without an applied electrolytic voltage. When the system is in equilibrium, its derivative concerning the

reaction coordinate disappears. Consequently, spontaneous reactions can only transpire when G decreases in the given conditions.

Determining the negative of the entropy, the expression for the first derivative of G with respect to T is:

$$\left(\frac{dG}{dT} \right) = -S \tag{2.4}$$

The formula for the second derivative of thermal capacity at constant pressure is:

$$\frac{d^2 G}{dT^2} = -\left(\frac{Cp}{T} \right) \tag{2.5}$$

Derivatives of this nature hold significant value in comprehending the thermodynamic characteristics and dynamics of a given system, specifically in the context of phase transitions, chemical reactions, and fluctuations in temperature and pressure. These tools find application in a wide range of disciplines, such as engineering, physics, and chemistry, to clarify and predict the behavior of substances under varying conditions [58].

3

DIELECTRIC SPECTROSCOPY

3.1 Dielectrics

A dielectric, or dielectric substance, functions as an insulating barrier that prevents the flow of electrical currents. When exposed to an electric field, it undergoes polarisation. However, in contrast to a conductive medium, electric charges within a dielectric substance stay immobile when exposed to an electric field. Instead, they experience subtle displacements from their balanced locations, resulting in a phenomenon referred to as dielectric polarisation [59].

The phenomenon of polarisation induces the displacement of positive charges in the direction of the electric field, whereas negative charges undergo movement in the opposite direction. For example, when the electric field is parallel to the positive x-axis, negative charges will be displaced in the opposite direction along the negative x-axis. As a result, this leads to the emergence of an internal electric field that reduces the overall strength of the field within the dielectric material. When a dielectric is made up of atoms that are weakly linked, In addition to polarisation, these particles reorient themselves so that they are symmetrically aligned with the applied electric field [60].

Understanding the mechanisms by which electric and magnetic energy are stored and distributed in materials. Dielectrics are essential for understanding and explaining many phenomena in the fields of electronics, optics, solid-state physics, and cellular biology [61]. The process of characterising a material, whether it is naturally occurring or artificially created, begins with the crucial step of accurately classifying its qualities. Of all these important characteristics, the ability to react to an external electric field is particularly notable. The phenomena being discussed is popularly known as conductivity, which categorises materials as conductors or insulators depending on their behaviour. This categorization determines whether a substance functions as an insulator when exposed to an external electric field.

Dielectric materials are materials that demonstrate polarisation when they interact with other substances [62]. Conductors are characterised by their many charges that may freely travel in any direction. These charges, which are mostly separate from and not attached

to nuclei, respond to an external electric field by promptly producing an electric current within the material [63]. Conversely, charges confined within dielectric materials stay strongly connected to their atoms, hindering their mobility and leading to little overall electric current. Within dielectric materials, these charges are limited to undergoing minuscule displacements alone in response to an external field.

An essential investigation in the whole evaluation of dielectric materials involves comprehending these little displacements and their correlation with the external field [64].

3.2 Dielectric Properties

Dielectric characteristics in liquid crystals pertain to the material's capacity to retain and convey electrical charges when subjected to an electric field. The qualities mentioned arise from the distinctive molecular alignment and polarisation behaviour displayed by liquid crystals under the influence of an electric field.

The application applying an electric field to a liquid crystal induces alignment of its rod-like or elongated molecules parallel to the direction of the field owing to their anisotropic characteristics. Consequently, the material undergoes alterations in the molecular dipole moments. Dipole moments indicate the spatial displacement of electric charges of opposite polarity within a molecule.

The degree of molecular alignment and polarisation in reaction to the electric field is contingent upon the particular phase of the liquid crystal and its molecular geometry. Distinct stages of liquid crystals display different dielectric reactions, leading to a range of electrical characteristics [65].

The dielectric constant, denoted as ε (epsilon), is a basic property of liquid crystals that describes their ability to store electrical energy. It quantifies the ability of a material to retain electrical energy when subjected to an electric field. A higher dielectric constant signifies an increased ability to retain electrical charges.

The manipulable dielectric characteristics of liquid crystals are very advantageous in the field of display technology, namely in LCDs. Electric fields may be utilised to change the alignment of liquid crystal molecules, resulting in accurate regulation of light transmission. This capability enables the generation of pictures and information that can be shown on LCD panels.

In addition to its use in display technology, liquid crystals also have many uses in sectors such as optoelectronics, sensors, and adaptive optics, due to its dielectric qualities. Scientists consistently investigate and manipulate liquid crystal materials to customise their dielectric properties for specific uses, hence enhancing the adaptability and usefulness of liquid crystals in contemporary technology [65].

3.3 Polarization

When a neutral atom is exposed to a continuous electric field E, it does not remain inactive as one might originally suppose. This is because atoms consist of a relatively large, An electrically charged nucleus with a positive charge is surrounded by a more pliable cloud of electrons that carry a negative charge. The response of these atomic components to the electric field is determined by their intrinsic properties [66]. In a more pronounced expression of this phenomenon, the contact might result in the whole elimination of atomic electrons, a phenomenon referred to as ionisation. This requires an electric field that exceeds the individual atom's threshold value. Nevertheless, captivating interactions are noticed when the threshold is exceeded.

The electric field, which exerts unequal forces on positive and negative charges, induces a polarisation that leads to an expansion of the distance between the poles. However, the interaction within the atom continues to exist, and a state of balance is achieved between the internal attractive force and the separation of charges caused by the external field. As a result, the atom undergoes polarisation as it aligns itself with the external field, resulting from the counteracting forces exerted on the positive and negative charges. The phenomenon of polarisation results in the creation of an atomic dipole moment, symbolised as μ, which is directly proportional to the external impact on the atom's outer area [67].

$$\mu = \alpha E \tag{3.1}$$

α in this equation represents the atomic polarizability, which is a distinct atomic property. Nevertheless, this approach, which is uncomplicated when used to individual atoms, becomes significantly more complex when dealing with compounds consisting of many atoms. Molecules exhibit varied levels of polarisation along different axes because of

their complex geometric shapes and physico-chemical properties. Therefore, when an electric field interacts obliquely with the relevant axis, it is necessary to determine the components of the field that are perpendicular and parallel to that axis before carrying out the computation. Hence, the dipole moment μ may be represented as the sum of α⊥E⊥ and α∥ E∥, taking into consideration both the perpendicular and parallel components [68].

Nevertheless, when dealing with materials lacking symmetry, which represents the most comprehensive case, it is necessary to modify this equation in order to accurately express the polarisation phenomena.

3.4 Dielectric Constant and Permeability

Empirical data shows that in many naturally occurring insulators, even in cases with exceptionally high fields, the resulting polarisation is directly proportional to the external field. This correlation is clearly established [69].

$$\mathbf{P} = \varepsilon_0 \chi_e \mathrm{E} \tag{3.2}$$

The given equation provides this formula, with χe denoting a dimensionless quantity known as the electrical susceptibility of the material. The magnitude of this component fluctuates depending on the particular substance and the external conditions in its environment.

By inserting the polarisation defined by including this approach into the calculation for electric displacement.

$$\mathbf{D}=\varepsilon_0 * \mathbf{E}+\mathbf{P}=\varepsilon_0 * \mathbf{E}+\varepsilon_0 * \chi_e * \mathbf{E}=\varepsilon_0 * \left(1+\chi_e\right) * \mathbf{E} \Rightarrow \mathbf{D}=\varepsilon \mathbf{E} \tag{3.3}$$

Available as.

$$\varepsilon=\varepsilon_0 * \left(1+\chi_e\right) \tag{3.4}$$

This number denotes the substance's electrical conductivity. When the susceptibility is equal to zero, the permittivity of vacuum is denoted as "ε_0" and is referred to as the "electrical permittivity of free space." Dividing both sides of this equation by "ε_0" results in a ratio that does not have any units.

$$\varepsilon_{r = 1+\chi_e} = \varepsilon/\varepsilon_0 \tag{3.5}$$

The term used to describe this phenomenon is known as the relative permittivity or dielectric constant of the material.

$$\mathbf{P}=\varepsilon_0\left(1+\chi_e\right)\mathbf{E} \tag{3.6}$$

It appears that this is really the situation. This formulation offers a more precise explanation of how the dielectric constant affects polarisation or the response of the dielectric material to an external electric field [70].

The equations obtained so far are defined in the MKS (meter-kilogram-second) or SI unit system. The subject is frequently addressed in the literature using the centimeter-gram-second (cgs) unit system. In the cgs system, the value of ε_0 is zero, which means that the relative permittivity (ε_r) is equal to the ε.

Starting here, because the equations are straightforward, the next chapters will use the cgs unit system.

3.5 Connected Loads and Electric Displacement

At this point, it becomes feasible to calculate the potential or electric field produced by a polarised dielectric medium. The emphasis lies on the field generated by the dipoles within the polarised material, rather than the field exerted on the material. To assess such a domain, one might simply start by examining the field generated by a single dipole. The final field created by the polarised material is determined by aggregating the effects of all dipoles [71].

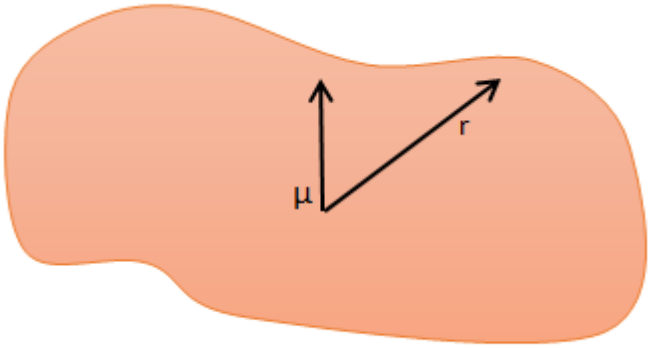


Fig 3.1 Calculating the polarisation of a dielectric substance and its corresponding surface area**.**

The electric potential generated by a dipole moment μ on the sample material, followed by the overall potential.

$$V(\mathbf{r})=\frac{1}{4\pi\varepsilon_0}*\frac{\mu}{r^2}*\hat{\mathbf{r}}\Rightarrow V_T(\mathbf{r})=\frac{1}{4\pi\varepsilon_0}*\int_v\frac{\mathbf{P}}{r^2}*\hat{\mathbf{r}}dv \tag{3.7}$$

can be expressed as in this context, the expression μ = Pdv is well recognised as the dipole moment within the volume element dv. The clarity of this integral can be enhanced by the utilisation of the product rules and the divergence theorem. The overall potential arising from the simplifications, it happens. At this point, we prioritise the divided components of the integral.

$$V_T(\mathbf{r})=\frac{1}{4\pi\varepsilon_0}*\left[\oint_s\frac{1}{r}*\mathbf{P}d\mathbf{a}-\int_v\frac{1}{r}*(\nabla\cdot\mathbf{P})*dv\right] \tag{3.8}$$

The overall potential arising from the simplifications, it happens. At this point, we focus our attention on the divided components of the integral.

Based on the above information, the first component may be understood as σb, which is equivalent to the surface charge potential represented by P. In the second part, ρ_b is

defined as the negative of ∇• P. The presence of a volume charge with a certain form is observed. Hence, the whole potential equation may be concluded accordingly.

$$V_T(\mathbf{r})=\frac{1}{4\pi\varepsilon_0} * \left[\oint_s \frac{\sigma_b}{r} * da+\int_v \frac{\rho_b}{r} * dv\right] \tag{3.9}$$

The discussion demonstrates that the region created by a polarised dielectric material is composed of the combined charge densities of both volume and surface. Due to the presence of these charges, specifically referred to as bound charges, it is possible to do computations on the regions formed by these interconnected charges instead of integrating across dipoles.

From this juncture, all consequences can be deemed applicable to the domain engendered by a polarised substance. In the case of a polarised dielectric, the impacts will be the combined result of the bound charges and the free charges, while considering the aforementioned explanation. Charges refer to unbound charges that exist outside the polarisation state inside a substance, such as ions. In this scenario, the overall charge in the material may be expressed as $\rho_f = \rho_b + \rho_f$, where ρ_f represents the free charges. Although this information may appear insignificant by itself, its primary significance is recognised in the context of Gauss's law or Maxwell's equations inside the content. Gauss's law "For a dielectric material $\varepsilon_0 \nabla \cdot E = \rho$ for a dielectric material

$$\varepsilon_0\nabla\cdot\mathbf{E}=\rho_b+\rho_f=-\nabla\cdot\mathbf{P}+\rho_f\Rightarrow\nabla\cdot(\varepsilon_0\mathbf{E}+\mathbf{P})=\rho_f \tag{3.10}$$

can be written. The expression in parentheses is defined as electric displacement and is denoted by the symbol D:

$$D=\varepsilon_0 E+P \tag{3.11}$$

Accordingly, Gauss's law is easily expressed by the equation $\nabla \cdot D = \rho_f$.

Although electric displacement (D) seems to be similar to electric field here, the two expressions should never be confused with each other. For there is neither a Coulomb's law of electric displacement nor, unlike E, the curl of D was always zero [72].

3.6 Fundamental Equations in Dielectric Theory

To assess the dielectric permittivity with respect to the actual dipole moment of insulating materials, it becomes imperative to ascertain the intrinsic field influencing the molecule and its polarizability – denoting the ratio between the dipole moment within the molecule and the collective average moments. This aspect has been extensively investigated by numerous researchers. However, given the comprehensive nature of this subject within systems, its thorough exploration falls beyond the confines of this thesis, thereby limiting this section to a succinct overview.

Fundamental relationships in static dielectric theory can essentially be expressed in a few equations. The first of these is the Claussius–Mossotti equation. This equation, which is valid for non-polar gases at low pressure, is also valid for the high frequency limit. The problem to be solved here is to calculate the dipolar contribution to polarizability:

$$\frac{\varepsilon-1}{\varepsilon+2}=\frac{4\pi N_A \rho \alpha}{3M} \tag{3.12}$$

Here M is the molecular weight, is the Avogadro number, and ρ is the density. The first solution to this problem for the static case is proposed by Debye with the contribution of distortional polarizability (α_d):

$$\frac{\varepsilon_s-1}{\varepsilon_s+2}\frac{M}{\rho}=\frac{4\pi}{3}N_A\left(\alpha_d+\frac{\mu^2}{3kT}\right) \tag{3.13}$$

This expression is the Debye equation for static permittivity, a generalization of the Clausius– Mossotti equation, and the left-hand side of the equation represents molar polarization. The expression "s" in the equation is the permeability at quiescent or low frequencies.

In these theories, the approaches use Lorentz fields. However, the Lorentz field loses its validity at some points, as it spontaneously predicts ferroelectricity. In the context of orientational polarization theory, an alternative solution to the local field problem comes from Onsager [54]. In the approach discussed, a spherical cavity with radius (a) and permeability of "1" is surrounded by a shell (b a) of radius much larger than its radius, and the permeability of this shell is 2. In addition, the cavity, together with its shell, is in a permeability 3 environment.

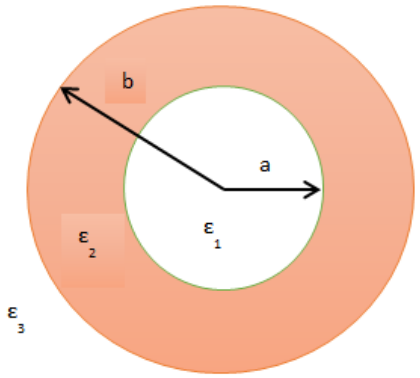


Fig 3.2 Spherical body with shell permeability "2" and core permeability "1" in a permeability medium "3".

Onsager equation as a result of various calculations made in this system

$$\frac{(\varepsilon_1-\varepsilon_\infty)(2\varepsilon_1+\varepsilon_\infty)}{\varepsilon_1(\varepsilon_\infty+2)^2}=\frac{4\pi N_1\mu_v^2}{9kT} \tag{3.14}$$

Available as. In the equation ε_∞ is the permeability at very high frequencies. Onsager studies dipolar orientation polarization on statistical grounds, just as Debye did. However, his approach for the gap here differs from Lorentz's, since the gap is assumed to be a dielectric material with macroscopic dielectric permeability. However, using the macroscopic argument to analyze the gap dielectric problem precludes consideration of local effects, which are important in condensed matter physics. This problem has been addressed by Kirkwoodand then by Fröhlich, briefly the range is surmounted by the development of a full statistical argument to determine the dipole–dipole interaction.

Dipole-dipole interaction, $\langle \mu \cdot \bar{\mu} \rangle = g\mu^2$, Kirkwood-Fröhlich equation,

$$\frac{(\varepsilon_1-\varepsilon_\infty)(2\varepsilon_1+\varepsilon_\infty)}{\varepsilon_1(\varepsilon_\infty+2)^2}=\frac{4\pi N_g \mu_v^2}{9kVT} \tag{3.15}$$

Is essentially a generalized version of the Onsager equation Here g is the correlation parameter, which is a measure of the local order in the material. In an infinite medium, the g-value is equal to 1 if the average momentum of a finite sphere surrounding a stationary molecule is the same as that molecule. In this case, there is no dipolar correlation between neighboring molecules or a dipole does not affect the positions and orientations of the neighbors. The value of g will be greater than 1 if the effect of the dipole directs the surrounding dipoles in the same direction, otherwise, i.e. in the opposite direction; the value of will be less than 1 [72].

3.7 Dielectric Relaxation and Cole–Cole Curves

In this chapter, relaxation, which is a unique dielectric behavior under time-dependent fields, will be discussed. In discussing this issue, Pellat's principle that after the appearance of a pre-existing field, the reduction of polarization in the absence of an electric field is independent of the dielectric's history and depends only on the value of the orientation polarization at that moment will be considered.

Since the proportionality constant corresponds to a time dimension, expressed by $1/\tau$, the following differential equation and its solution for orientation polarization in the absence of the electric field are,

$$\dot{\mathbf{P}}(t)=-\frac{1}{\tau}\mathbf{P}(t)\Rightarrow \mathbf{P}(t)=-\frac{1}{\tau}\mathbf{P}_0 e^{-t/\tau} \tag{3.16}$$

Is obtained as follows. In this case, the step–response function of the orientation polarization is

$$\alpha_p(t) = e^{-t/\tau} \tag{3.17}$$

It is given with an exponential decay such that here, the time constant τ is called the relaxation time [73]. The Debye approach is one of the simplest expressions that can be used to describe experimental relaxation data [74]. This equation can also be defined as a single relaxation time.

3.8 Cole–Cole Equation

The first alternative empirical equation to the Debye type or one-time relaxation equation was also proposed by the Cole and Cole duo. Accordingly, the complex dielectric constant is given as. Here, α takes values between 0 and 1, and it can be clearly seen that when α = 0, this equation reverts to the Debye equation. For this reason, the Cole–Cole equation can be easily preceded in experimental analyzes. Because, in cases where the system exhibits Debye-type relaxation, the value of α will take a magnitude close to 0 or very close to zero [75].

$$\varepsilon^{*}(\omega)=\varepsilon_{\infty}+\frac{\varepsilon_s-\varepsilon_{\infty}}{1+(i\omega\tau)^{1-\alpha}}| \tag{3.18}$$

According to equation (3.18), the real part of the complex dielectric constant is:

$$\varepsilon^{'}(\omega)=\varepsilon_{\infty}+(\varepsilon_s-\varepsilon_{\infty})\frac{1+(\omega\tau)^{1-\alpha}\sin\frac{1}{2}\alpha\pi}{1+2(\omega\tau)^{1-\alpha}\sin\frac{1}{2}\alpha\pi+(\omega\tau)^{2(1-\alpha)}} \tag{3.19}$$

And the virtual part,

$$\varepsilon^{''}(\omega)=(\varepsilon_s-\varepsilon_{\infty})\frac{1+(\omega\tau)^{1-\alpha}\cos\frac{1}{2}\alpha\pi}{1+2(\omega\tau)^{1-\alpha}\sin\frac{1}{2}\alpha\pi+(\omega\tau)^{2(1-\alpha)}} \tag{3.20}$$

Are equal to their equations. In the experimental measurements, the experimental relaxation data of the relevant material can be analyzed by fitting these functions [76].

3.9 Temperature-Related Measurements and Activation Energy

The dependence of the complex dielectric constant of a dielectric material, namely its electrical permittivity and conductivity, in these sections, besides explaining that the dielectric constant is dependent on angular frequency and permeability. It has been clearly shown by the mentioned basic equations that the temperature of the material is also a function [77].

In 1889, Svante Arrhenius proposed the Arrhenius equation, which is named after him, based on his observations on the graphs of rate constants and temperatures. With the help of this equation, the activation energy of the relevant sample can be calculated. Here, the activation energy (E_a) can be defined, as the minimum energy required the molecule to contribute to the conductivity. If the Arrhenius equation is written over the conductivity,

$$\sigma=\sigma_0 \exp\left(-\frac{E_a}{k_B T}\right) \tag{3.21}$$

In this equation, k_B is Boltzman's constant and its value is 8.6173303×10^{-5}. It is equal to the magnitude $eV \cdot K^{-1}$. Likewise, σ_0 is the exponential coefficient and T is the temperature in Kelvin [78].

The complex dielectric permittivity depending on angular frequency and temperature, the activation energy of the experimentally determined material, can be calculated with Arrhenius plots drawn using the Arrhenius equation. If the equation (3.22) is considered again for the graphs in question, as in the previous section, when the logarithm is taken for both sides of the equation .

$$ln\,\sigma = -\frac{E_a}{k_B}\frac{1}{T} + ln\,\sigma_0 \tag{3.22}$$

Again, this equation will be a first-order equation, such as $y = -mx + b$, with $y = \ln\sigma$, $x = 1/T$ and $\ln\sigma_0$ a constant. So, if the temperature dependent ln σ data derived from the experimental results are plotted against the 1/T values, the slope of the resulting graph will be equal to the value Ea/k_B [79].

Arrhenius plots are usually plotted against 1000/T values for a more convenient visualization. Because the 1/T values of the selected temperatures in the measurements made, usually have very small values around the room temperature. Therefore, the values are multiplied by 1000 to rank them as natural numbers. Generally, high frequency ranges are chosen when making dielectric measurements of a material. Therefore, results are obtained against a large number of frequencies. However, in temperature-dependent measurements, relatively few measurements are taken relative to frequency. In these measurements, unlike other terms, the activation energy contains a temperature-dependent data set for each frequency. This means that there is a large amount of data that can be calculated. Calculations are therefore usually made against selected frequencies, not against all frequencies [80].

.

4
MATERIAL AND METHOD

4.1 Materials

4-Cyano-4'-pentylbiphenyl (**5CB**) is a frequently utilized nematic liquid crystal represented by the chemical formula C18H19N. It is commonly known as **5CB** [81]. The pioneering synthesis of **5CB** occurred in 1972 at the University of Hull by George William Gray, Ken Harrison, and J.A. Nash. This marked the inception of the cyanobiphenyls class. The revelation of this liquid crystal came about through a research grant from the UK Ministry of Defence, which aimed to discover liquid crystals featuring phases near room temperature for potential application in liquid crystal displays. The molecular length of **5CB** is approximately 20 Å. Notably, **5CB** experiences a phase transition from crystalline to nematic at 22.5 °C and further transitions from a nematic to an isotropic state at 35.0 °C.

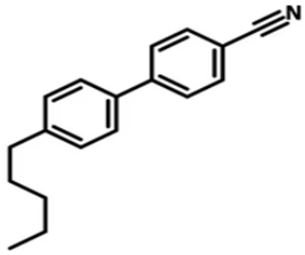


Fig 4.1 Chemical structure of 4-Cyano-4'-pentylbiphenyl (**5CB**).

The synthesis of **5CB** involves sequential modifications to biphenyl in a linear fashion. To initiate the process, Br2 is incorporated into the biphenyl structure, attaching a bromine atom to one end. Subsequently, a mixture of aluminum chloride and C4H9COCl is introduced, followed by the addition of potassium hydroxide and NH2NH2. These steps lead to the formation of a molecule with a bromine atom on one extremity of the rigid core and C5H11 on the opposite end. The final step entails the utilization of copper (I) cyanide and DMF, resulting in the substitution of the bromine atom with a CN group. This series of reactions ultimately yields the creation of **5CB** [82]. The electrical conductivity of a material primarily relies on its temperature and resistance. In the context of liquid crystals, the conductivity increases due to the presence of residual ionic impurities. The anisotropic conductivity is determined by these factors [83].

LC1: (S)-4-n-octyloxybenzylidene-4'-(3, 7-dimethyloctyloxy) aniline

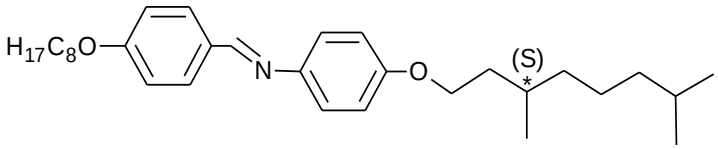


Fig 4.2 The molecule structure of **LC1**.

LC2: (*S*)-5-*n*-octyloxy-2-[[[4'-(3,7dimethyloctyloxy) phenyl] imino] methyl] phenol

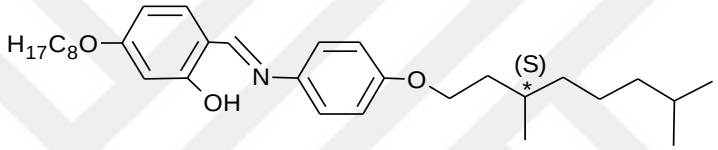


Fig 4.3 The molecule structure of **LC2.**

4.2 Preparation of LC Cells

Empty cells have been prepared by indium-tin-oxide (ITO) coated glass plates purchased by Instec Colorada Inc. (Fig. 4.4).



Fig 4.4 Empty cells (indium-tin-oxide (ITO) coated glass plates).

The thickness of the empty cells was set as d=9±0.1 μm by Mylar spacer. We have prepared cells with planar orientation which was provided by a rubbed layer of polyimide. Before filling the cell with **5CB**, **5CB+ (1%) LC1** and **5CB+ (1%) LC2** the capacitance of the empty cell, C_{air}, has been measured by HP 4192A Impedance Analyzer. The ITO

cells have been filled with the **5CB**, **5CB+ (1%) LC1** and **5CB+ (1%) LC2** by capillary action (Fig. 3.7) .



Fig 4.5 Schematic representation of injecting the sample into the cell.

4.3 Devices and Equipment Used

Dielectric impedance analyzer: Dielectric spectroscopy (DS) or impedance spectroscopy (ES), also referred to as electrochemical impedance spectroscopy, is a widely employed technique for investigating how a sample responds when subjected to an electric field of consistent or varying frequency. This method provides insights into the dielectric characteristics of a material in relation to the frequency [84].

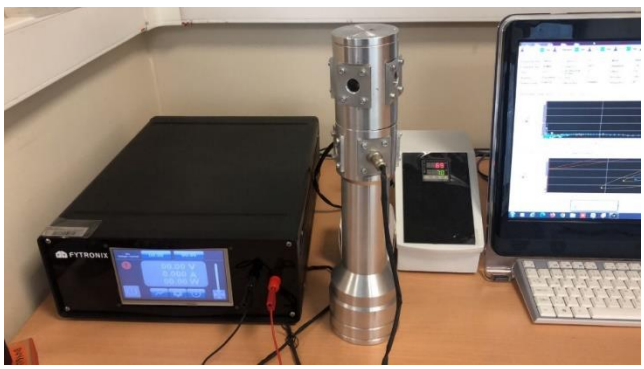


Fig 4.6 Schematic representation of Impedance Analyzer.

The Impedance Analyzer is utilized to measure a range of parameters including Capacitance/Dielectric Constant, Inductance, Resistance, Impedance, Dissipation factor, and Quality factor.

Temperature Controller:

A Temperature Controller functions as a tool employed to regulate a heater or similar apparatus. It achieves this by contrasting a sensor signal against a predetermined set point and executing calculations based on the disparity between these measurements. Controllers that are capable of managing sensor signals beyond temperature, encompassing aspects like humidity, pressure, and flow rate, fall under the category of Controllers. When these controllers operate in electronic form, they are specifically referred to as Digital Controllers [85].



Fig 4.7 Schematic representation of temperature Controllers device.

Temperature Controllers function to maintain the process value at the designated set point, although the manner of response can vary due to the distinct characteristics of the controlled entity and the specific control methodology employed by the Temperature Controller [86].

Kofler Bank:

A Kofler bank serves as a laboratory tool employed in chemistry to ascertain the melting points of various chemical compounds. Its structure involves an elongated rectangular block, usually constructed from metal or glass, which is subjected to control heating spanning from one end to the other [87].



Fig 4.8 Schematic representation of Kofler bank device.

This apparatus is typically etched with a series of equidistant temperature gradients, facilitating the determination of a substance's melting point through observation of the point at which it initiates melting and forms a liquid droplet. This data proves valuable for the identification of unknown substances; as distinct chemical compounds possess unique melting points.

The Kofler bank derives its name from its inventor, Heinrich Kofler, a German chemist who crafted the device during the early 20th century. It remains widely employed in contemporary chemical analysis and research, especially within the realms of organic chemistry and pharmaceutical studies [88].

Cryostat:

A cryostat functions as a specialized apparatus employed to uphold exceedingly low temperatures for scientific experiments or industrial processes. Essentially, it constitutes a chamber intricately designed to sustain its contents within an extremely cold range, typically spanning from just a few degrees above absolute zero (-273.15°C or -459.67°F) to temperatures substantially below freezing.



Fig 4.9 Schematic representation of cryostats device

These cryostats find widespread use in fields like physics, chemistry, and materials science, where the examination of material and particle behavior necessitates the application of low temperatures. Moreover, they have significant applications in medical and industrial domains, contributing to endeavors like semiconductor manufacturing and the generation of superconducting magnets.

Cryostats come in diverse forms, encompassing closed-cycle and open-cycle variations. Closed-cycle cryostats employ a self-contained system of refrigerants to sustain the low temperatures, while open-cycle cryostats employ coolants like liquid nitrogen or helium. Additionally, these cryostats can incorporate various attributes such as vacuum insulation,

radiation shields, and magnetic shielding, all of which contribute to precise environmental control within the chamber.

In essence, cryostats serve as pivotal tools across numerous scientific and technological domains, empowering researchers and engineers to meticulously study and manipulate materials under conditions of exceptional coldness [89]

5
RESULT AND DISCUSSION

5.1 Mesomorphic Properties of LC1 and LC2

The chemical structures of the **5CB**, **LC1** and **LC2** have been shown in Fig.5.1.

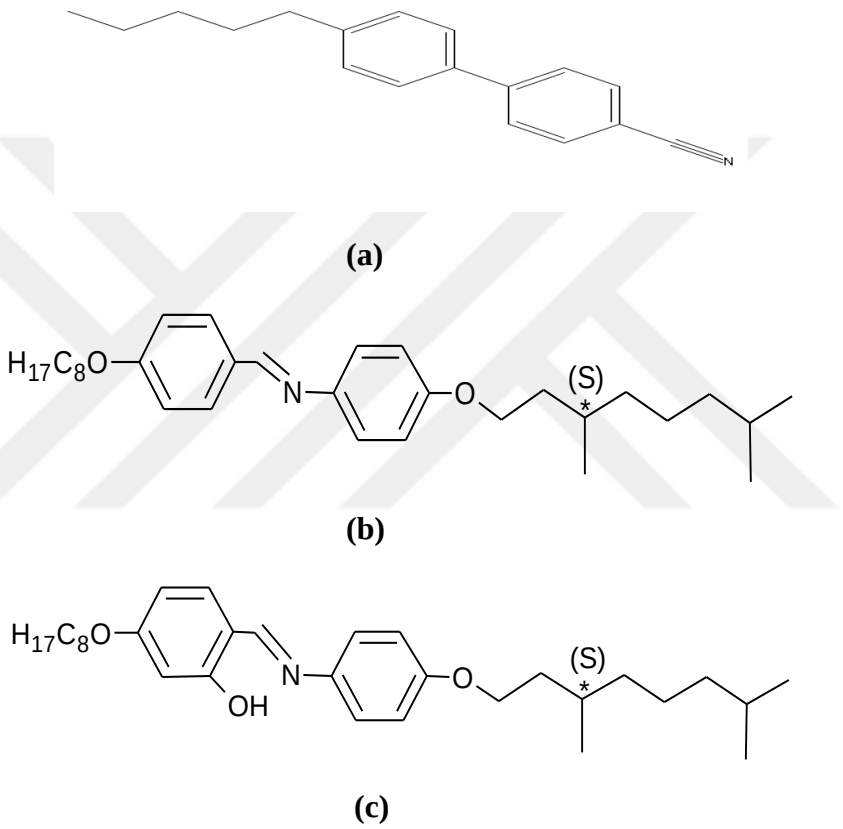


Fig 5.1 The Chemical structures of the (a) **5CB**, (b) **LC1** and (c**) LC2**.

Figure 5.2 show us during the heating process for **LC1** we can notice that at 74.25 ^{o}C there is phase transtion for Cr to SmC* and when measuring the value of enthalpy we get

34.50 kJ/mol and when the temperature ıs reached to 78.80 ºC we wıll get phase transtion for SmC* to Iso and the value of enthalpy for this state is 5.26 kJ/mol.

For the cooling process we have a phase transition from Iso to SmC* phase at 77.45 ºC and the enthalpy is 5.32 kJ/mol and when we get 57.85 ºC a phase transition will occur from SmC* to Cr then the value of the enthalpy will be 17.59 kJ/mol.

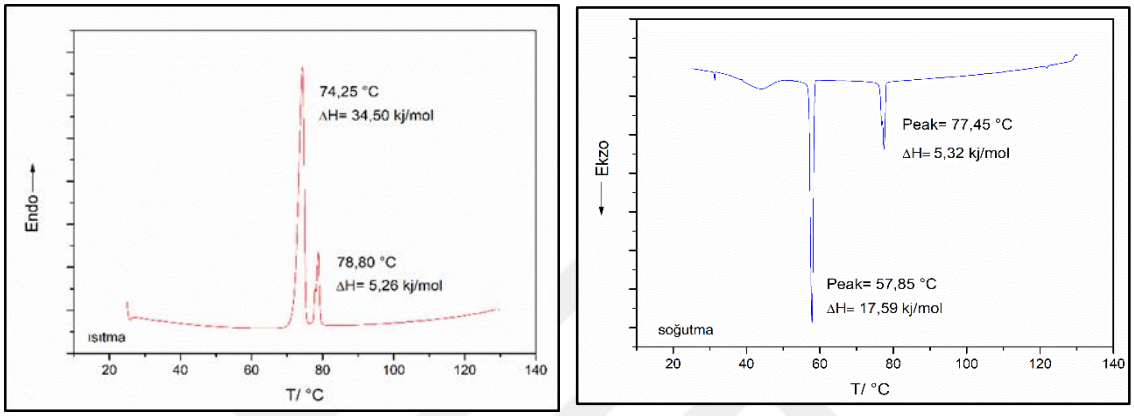


Fig 5.2 DSC thermograms of compound **LC1** on 2nd heating and cooling (10 °C min^{-1}).

Figure 5.3 show us during the heating process for **LC2** we can notice that at 53.59 ºC there is phase transtion for Cr to SmC* and when measuring the value of enthalpy we get 33.34 kJ/mol and when the temperature ıs reached to 86.62 ºC we wıll get phase transtion for SmC* to Iso and the value of enthalpy for this state is 8.96 kJ/mol .For the cooling process we have a phase transition from iso to SmC* at 85.15 ºC and the enthalpy is 8.82 kJ/mol and when we get 29.52 ºC a phase transition will occur from SmC* to Cr then the value of the enthalpy will be 16.51 kJ/mol. That is means we get phase transition at this point, which change sharply.

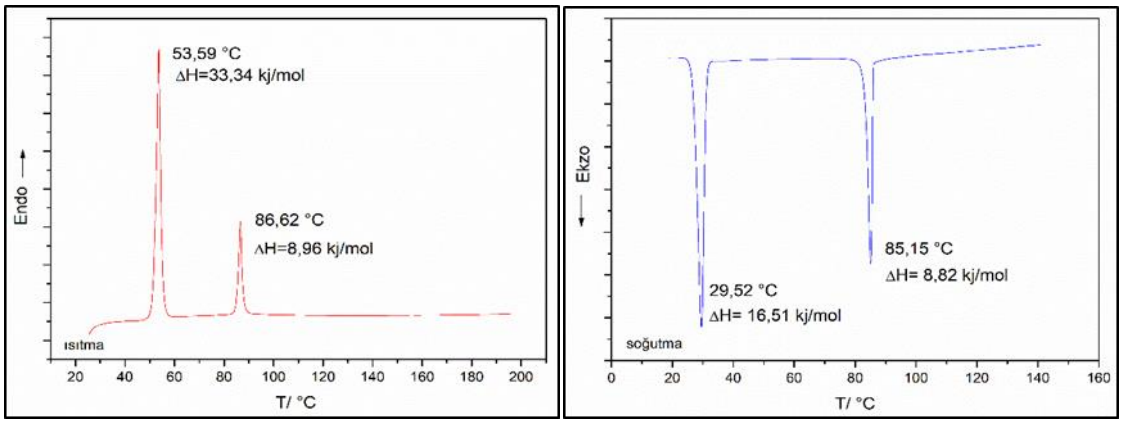
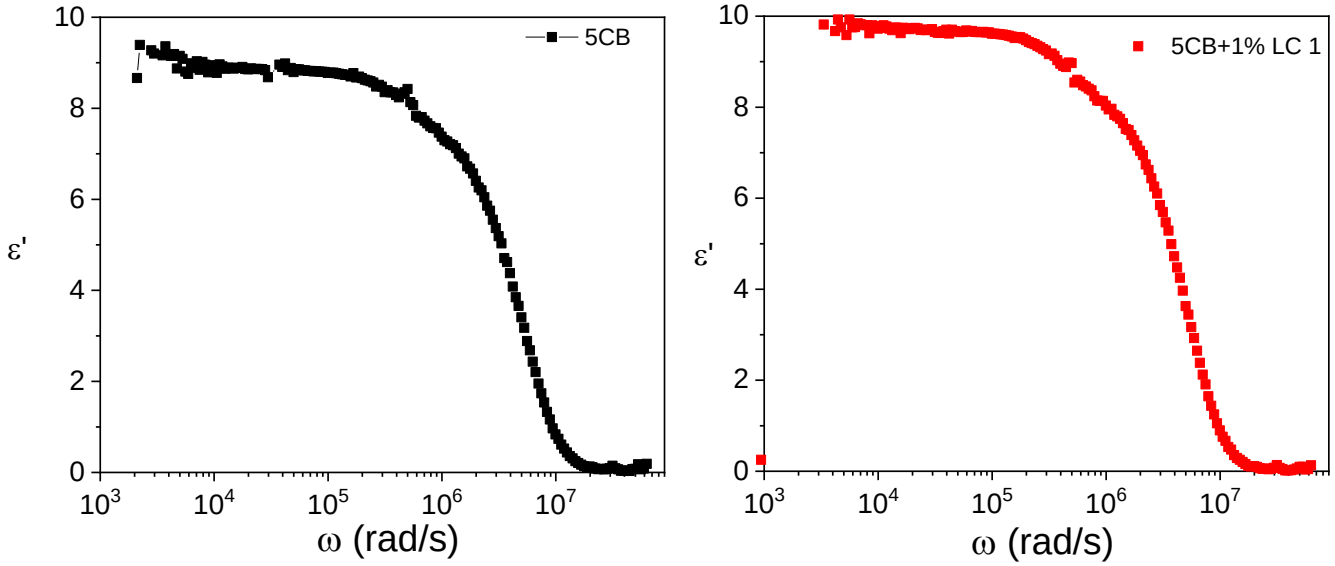


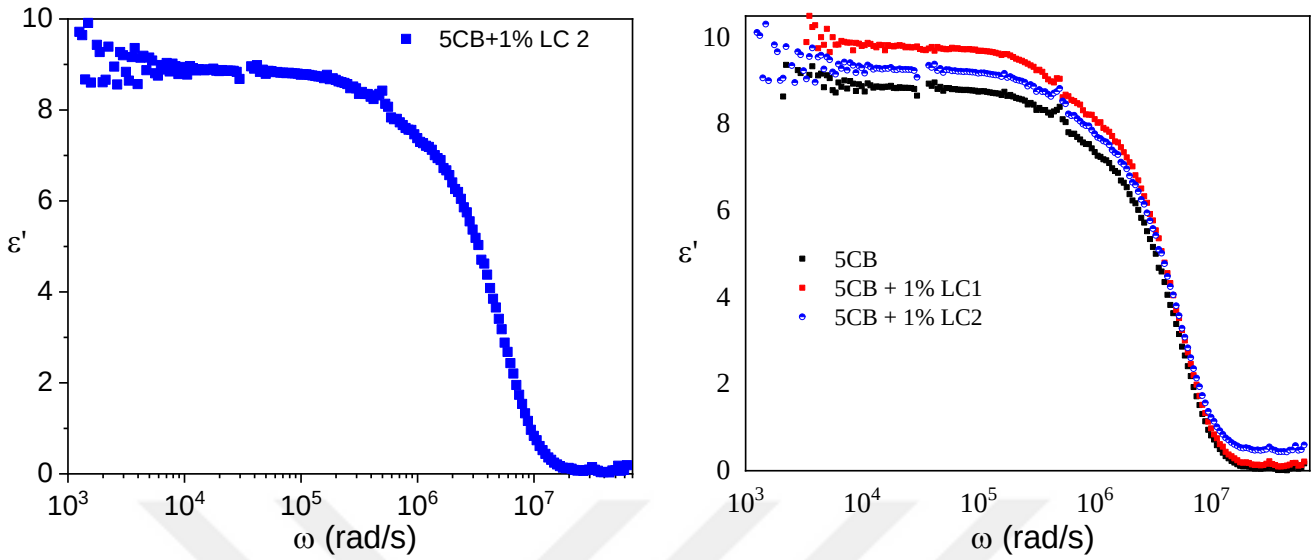
Fig 5.3 DSC thermograms of compound **LC2** on 2nd heating and cooling (10 °C min^{-1}).

5.2. Dielectric Parameters of 5CB, 5CB+ 1%LC1 and 5CB+ 1% LC2

Dielectric parameters of Liquid crystal were measured by Fytronix Impedance Analyzer in the frequency range of 100Hz-10MHz. The frequency dependencies of the real and imaginary parts of the dielectric constant of **5CB**, **5CB+ 1% LC1** and **5CB+ 1% LC2**, which can be seen in Figure 5.4 and Figure 5.5, respectively.

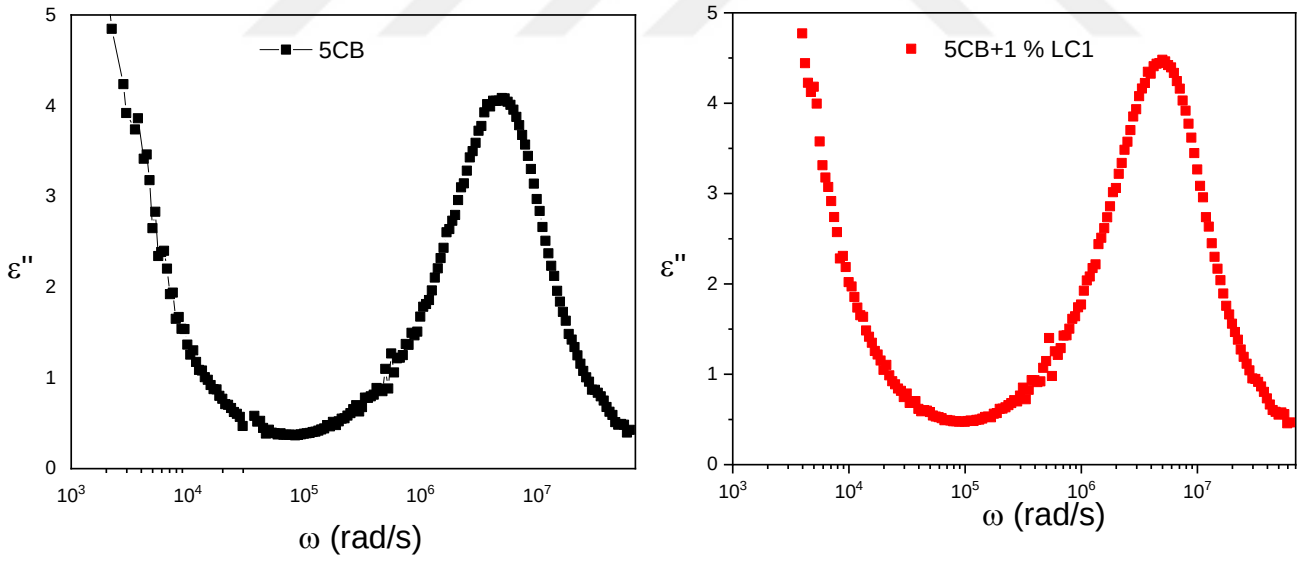


(a) (b)

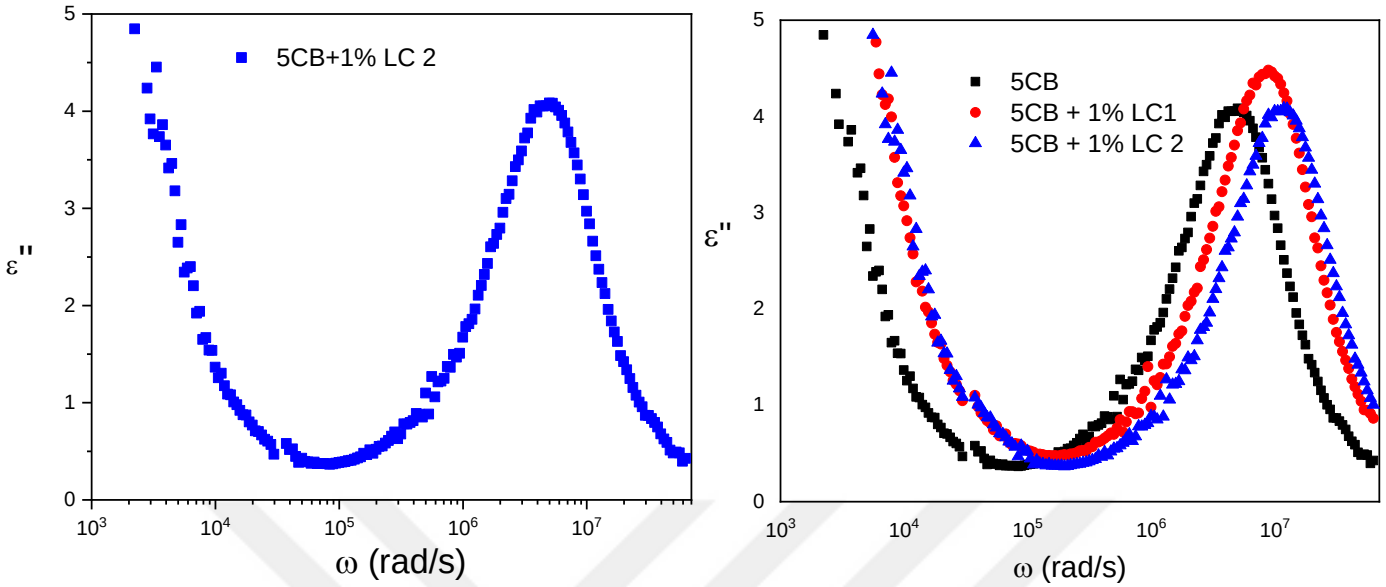


(c) **(d)**

Fig 5.4 The real component of the dielectric constant versus angular frequency for (a) **5CB** (b) **5CB+1% LC1** (C) **5CB+1% LC2** (d) comparative results.



(a) *(b)*



(c) **(d)**

Fig 5.5 The results for imaginary components of the dielectric constant (a) **5CB** (b) **5CB+1%LC1 (C) 5CB+1%LC2** (d) comparative results

The first thing to note here is that the values of the complex dielectric constant change depending on frequency, as expected. As can be clearly seen from the Figure 5.4, the real part of the dielectric constant decreases when the frequency increases, and on the other hand, it has its maximum value at low frequencies. On the contrary, in the imaginary part, the values, which are generally high at low frequencies, then increase again at high frequencies and pass through a peak (Fig.5.5).

The appropriateness of the selected model can be assessed by examining Cole-Cole curves, which represent how the components of the complex dielectric constant vary in relation to one another. In Figure 5.6 the Cole-Cole curves for **5CB**, **5CB+ (1%) LC1**, and **5CB+ (1%) LC2** liquid crystals are shown. These curves closely resemble Debye curves, taking on a semicircular shape. Additionally, the a values resulting from the fitting process are extremely close to zero, serving as strong evidence of this Debye-like behavior. In conclusion, it can be stated that the fits performed and the parameters obtained from the fitted curves strongly suggest that the **5CB**, **5CB+ (1%) LC1**, and

5CB+ (1%) LC2 liquid crystals exhibit a relaxation curve consistent with the Debye model.

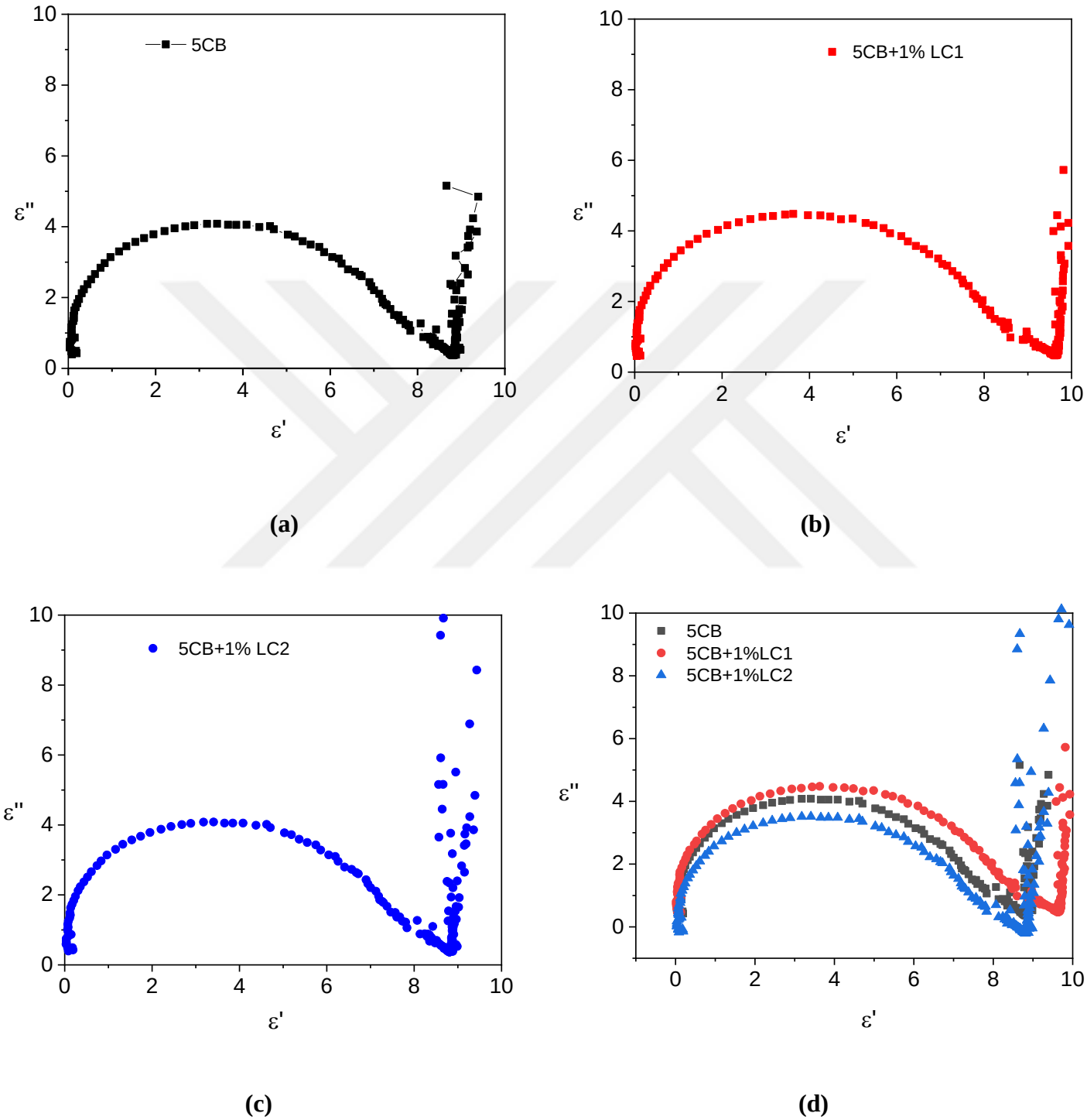


Fig 5.6 The Cole – Cole plots of (a) **5CB** (b) **5CB+1%LC1** (C) **5CB+1%LC2** (d) comparative results.

As indicated in figure (5.6), the absorption coefficients exhibit an increase when doping is applied in both the first (low-frequency) and the second relaxation (high-frequency) regions. However, the addition of **1% LC1** and **1% LC2** to **5CB** leads to a significant exponential decrease in the α coefficient. This reduction approaches zero, aligning with the Debye model, particularly for the high-frequency region and under high DC bias conditions. Moreover, the introduction of **1% LC1** and **1% LC2** into **5CB** results in a decreased time constant for the high-frequency region. Since a lower time constant is associated with doping, it signifies that the reorientation of molecules commences at a lower threshold voltage in comparison to pure **5CB**.

5.2. AC Conductivity of the Liquid Crystal Composites (5CB, 5CB+ 1% LC1 and 5CB+ 1% LC2)

The AC conductivity of composites containing liquid crystals, denoted as σ_{ac}, has been computed using the formula 5.1,

$$\sigma_{ac} = \omega\, \varepsilon_0\, \varepsilon'' \tag{5.1}$$

The equation involves the representation of angular frequency as ω and the dielectric constant of empty space as ε_0. And ε" represents the component regarding the dielectric constant that is imaginary. Figure 5.7 (a, b, and c) illustrates the variations in The relationship between the natural logarithm of σac and the natural logarithm of angular frequency (ln σac with ln ω) is examined for three substances: **5CB, 5CB+ (1%) LC1, and 5CB+ (1%) LC2**. Figure 5.7 (c) demonstrates the impact of including **1% LC1** and **1% LC2** on the AC conductivity of the samples.

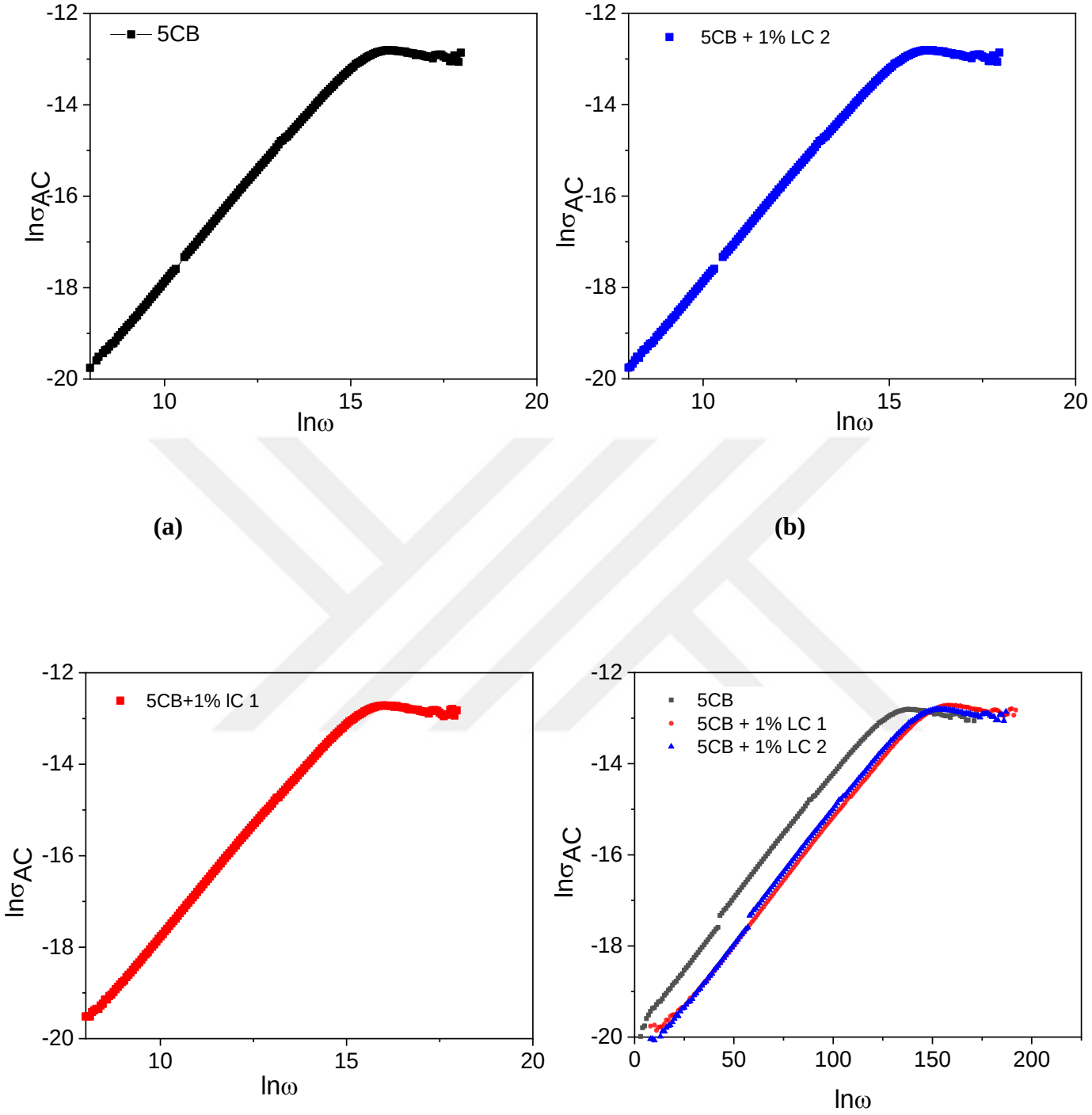


Fig 5.7 The variation of ln σ_{AC} with angular frequency for (a) **5CB** (b) **5CB+1%LC1** (c) **5CB+1%LC2** (d) comparative results.

The conductivity of **5CB**, **5CB+ 1% LC1**, and **5CB+ 1% LC2** at both low and high frequencies has been measured, revealing several forms of frequency-dependent behavior.

5.3 Dielectric Parameters of LC1 Liquid Crystal at various temperatures

An investigation was conducted on the dielectric properties of **LC1** liquid crystal throughout a temperature range of 28°C to 92°C, which included phase transition temperatures. The investigation also included a frequency range from 100Hz to 10MHz. Figures 5.8 and 5.9 illustrate how the real and imaginary parts of the dielectric constant for **LC1** change with frequency.

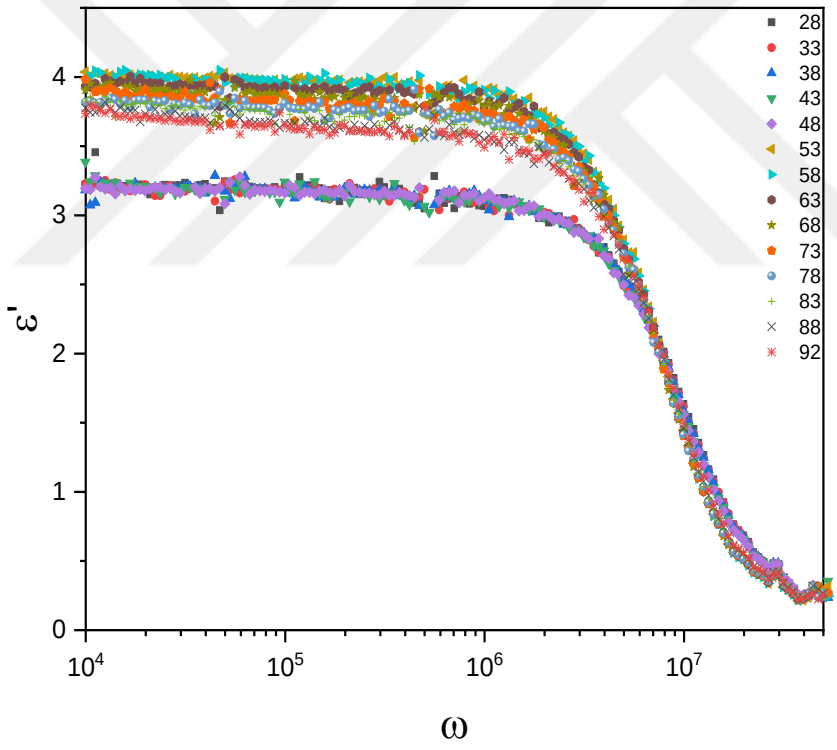


Fig 5.8 The real component depend on angular frequency of **LC1** at different temperatures (28 – 92ºC).

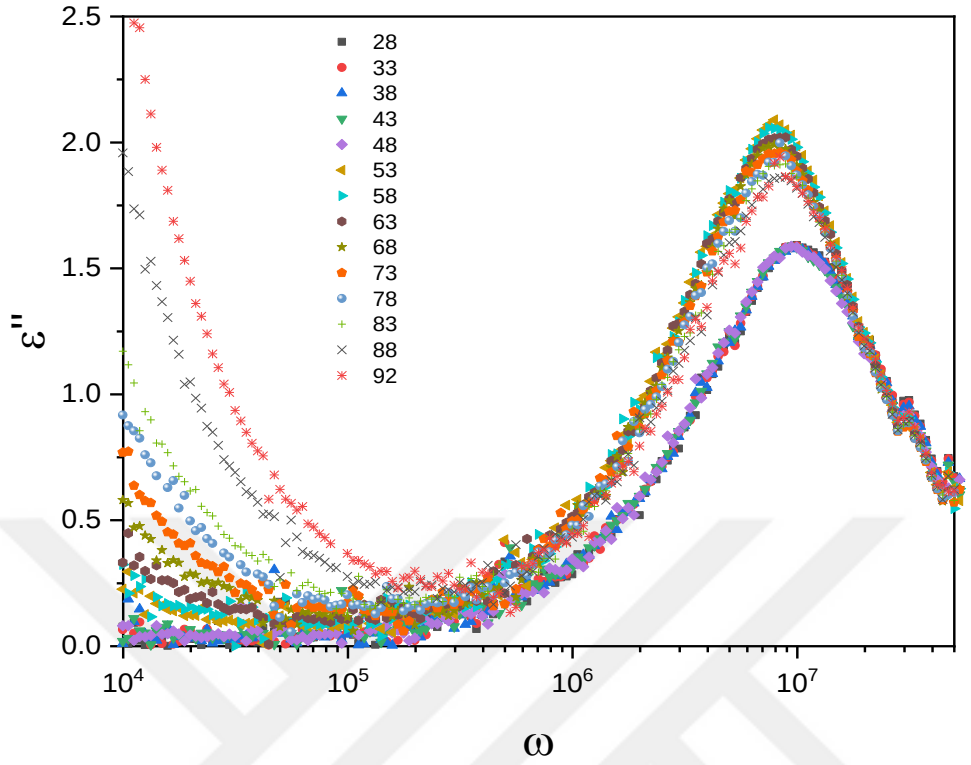


Fig 5.9 The imaginary component depend on angular frequency of **LC1** at different temperatures (28 – 92ºC).

It is crucial to acknowledge that, as expected, the complex dielectric constant values fluctuate with temperature and frequency changes. The graphs demonstrate a reduction in the fundamental component of the dielectric constant as the frequency increases, with the highest value observed at low frequencies. In contrast, the imaginary portion has elevated values at lower frequencies, then increases again at higher frequencies, resulting in a peak. The fundamental component exhibits a progressive increase with temperature, followed by a reduction following the phase change at 78°C. The temperature-dependent impact is seen in the fluctuations of the dielectric constant at specific frequencies as the temperature changes.

The chosen model's suitability may be assessed by employing Cole-Cole plots, one may visually represent the relative fluctuations in the elements of the complex dielectric constant. The **LC1** liquid crystal is depicted in Figure 5.10 using Cole-Cole graphs at

various temperatures ranging from 28°C to 92°C. The form of these curves closely approaches Debye curves, exhibiting a semicircular appearance.

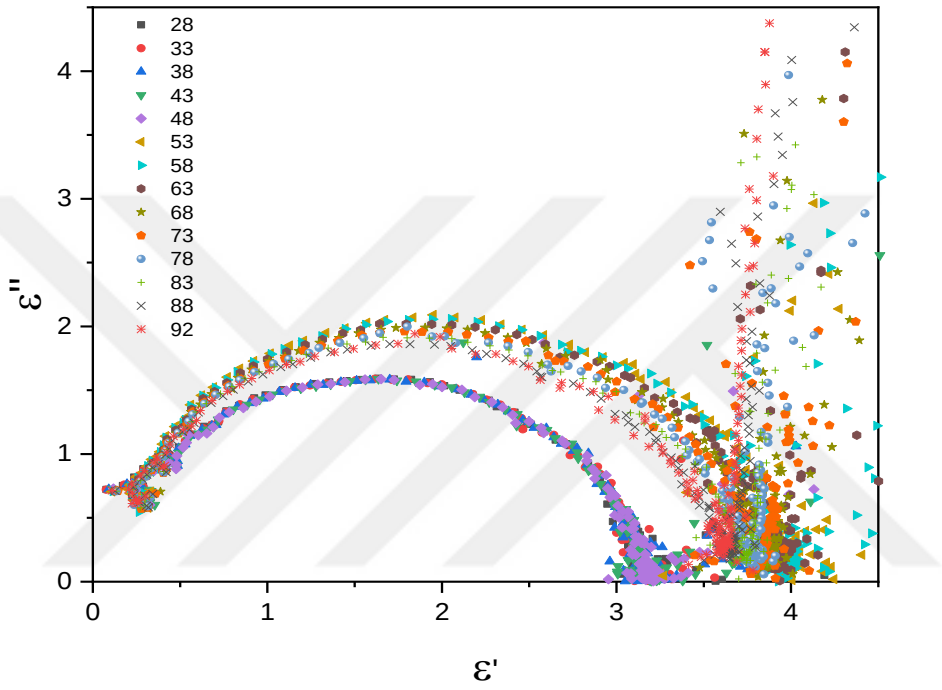


Fig 5.10 The Cole – Cole curve of **LC1** at different temperatures.

The evidence clearly indicates that the molecule undergoes readily recognisable phase transitions. Therefore, it is justifiable to claim that the data obtained using Dielectric Spectroscopy may be used to enhance the measurement of phase transition temperatures.

5.3. AC Conductivity of the LC1 at Various Temperatures

The determination of conductivity processes in the **LC1** was based on the observed ε" values, as described in Section 5.2.1. The ln σac values were determined for each temperature ranging from 28°C to 92°C. The relationship between the logarithm of σ_{ac} and the logarithm of angular frequency (ln σ_{ac} with ln ω).

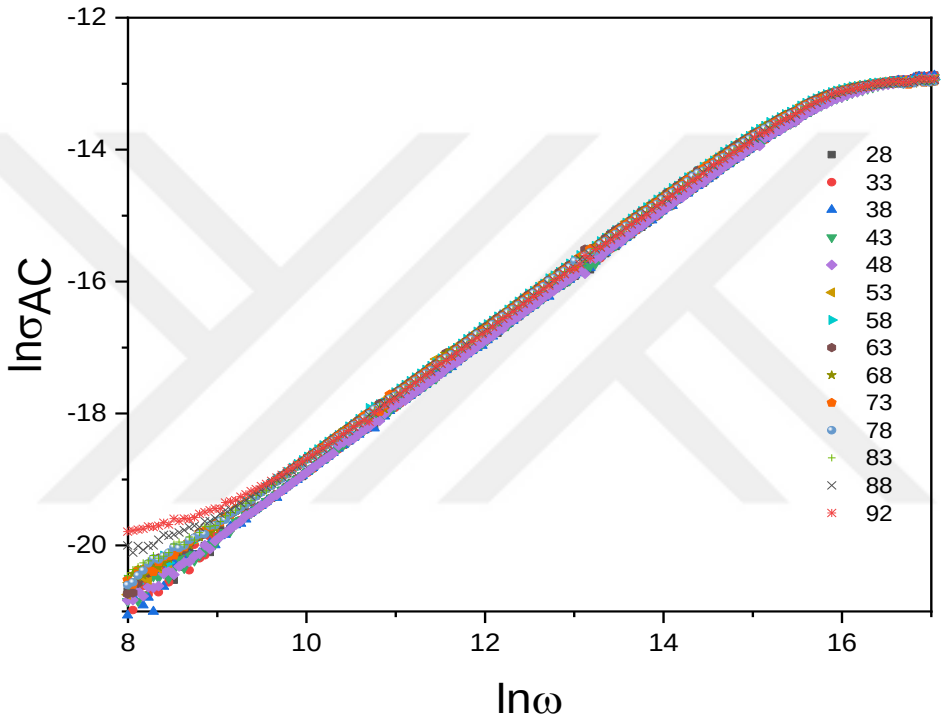


Fig 5.11 ln σAC versus lnω graphics of **LC1** at different temperatures.

The creation process involved the careful selection of the mechanics. The graph shows that conduction processes exhibit minimal variation with temperature throughout the applicable frequency ranges. Mechanism differentiation only happens inside the high-temperature and high-frequency range.

In Fig 5.12, the relationship between the natural logarithm of the electrical conductivity ($\ln\sigma_{AC}$) and the reciprocal of temperature (1000/T) is displayed for specific chosen frequencies. According to Figure 5.12, conductivity generally increases as frequency increases. As the temperature lowers, the natural logarithm of the electrical conductivity

of AC decreases. Based on this perspective, it may be inferred that there is a thermally triggered mechanism for the movement of the charge carriers.

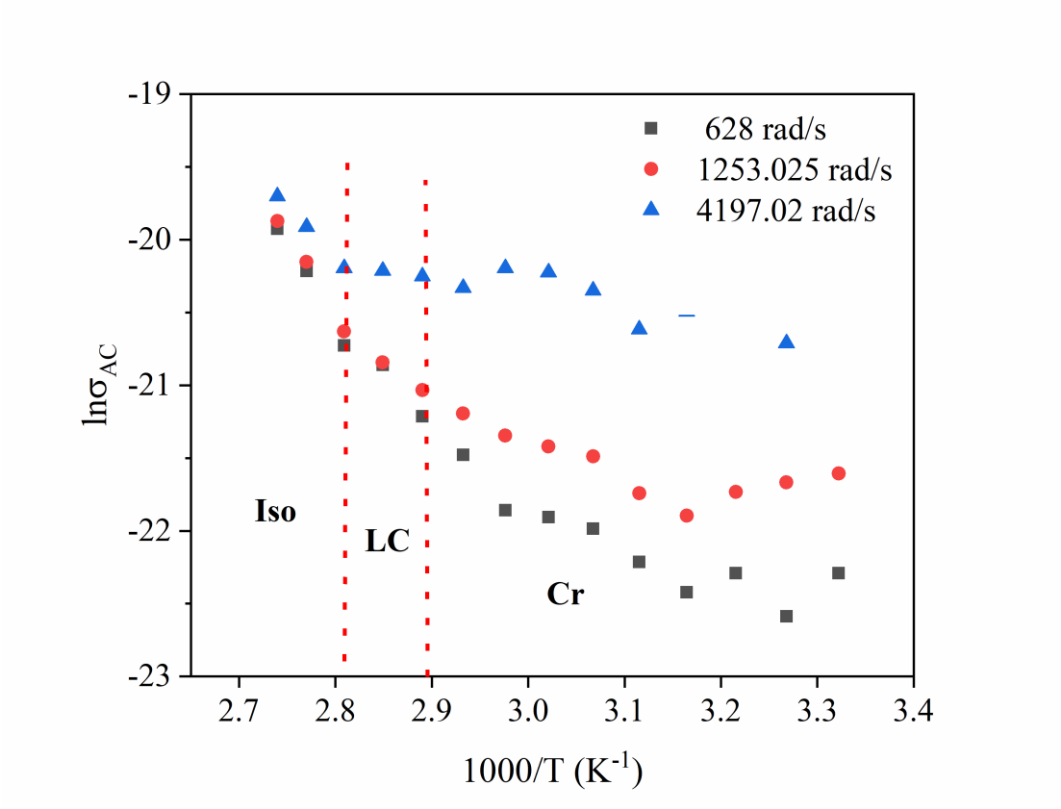


Fig 5.12 The Temperature dependence of $\ln\sigma_{AC}$ versus 1000/T of **LC1** for ω=628 rad/s, ω=1253.025 rad/s and ω=4197.02 rad/s.

6
CONCLUSIONS

In the study, the dielectric properties of **5CB, 5CB+ 1%LC1** and **5CB+1%LC2**, were examined at room temperature and the dielectric properties of **LC1** were examined at different temperatures. An analysis was conducted on the dielectric constant's real (ε') and imaginary (ε") components throughout a frequency spectrum spanning a frequency range of 100 Hz to 10 MHz. The dielectric relaxation seen in these liquid crystal systems was evaluated using Cole-Cole plots, indicating two separate dielectric relaxation processes. Significantly, including **LC1** in **5CB** led to increase the size of the Cole-Cole plot diameters whereas including **LC2** in **5CB** led to decrease the size of the Cole-Cole plot diameters.

The inclusion of **LC1** and **LC2** in **5CB** accelerated the reorientation of molecules. Manipulating the doping concentration in this system can lead to a desirable molecular arrangement in devices, which is especially beneficial for electro-optic applications.

The **LC1** liquid crystal is depicted using Cole-Cole graphs at various temperatures ranging from 28°C to 92°C. The form of these curves closely approaches Debye curves, exhibiting a semicircular appearance. The evidence clearly indicates that the molecule undergoes readily recognisable phase transitions. Therefore, it is justifiable to claim that the data obtained using Dielectric Spectroscopy may be used to enhance the measurement of phase transition temperatures.

REFERENCES

[1] I. Dierking, S. Yoshida, T. Kelly, and W. Pitcher, “Liquid crystal-ferrofluid emulsions,” *Soft Matter*, vol. 16, no. 26. Royal Society of Chemistry, pp. 6021–6031, Jul. 14, 2020. doi: 10.1039/d0sm00880j.

[2] S. Park, Y. Oh, J. Moon, and H. Chung, “Recent Trends in Continuum Modeling of Liquid Crystal Networks: A Mini-Review,” *Polymers (Basel).*, vol. 15, no. 8, 2023, doi: 10.3390/polym15081904.

[3] E. Adamovich *et al.*, “Towards Femtoscan-Assisted Analysis of Liquid Crystal Self-Organization on Different Polymer and Glass Surfaces for Lab-on-a-Chip and Lab-on-a-Dish Applications, Including Optofluidic and Flexoelectric Ones,” *Recent Prog. Mater.*, vol. 05, no. 02, pp. 1–24, 2023, doi: 10.21926/rpm.2302022.

[4] D. Kalinin and J. Abercrombie, “The Applications of Machine Learning in the Study of Liquid Crystals: A Review,” *J. Student Res.*, vol. 12, no. 1, pp. 1–16, 2023, doi: 10.47611/jsrhs.v12i1.3983.

[5] Z. Wen, K. Yang, and J. M. Raquez, “A review on liquid crystal polymers in free-standing reversible shape memory materials,” *Molecules*, vol. 25, no. 5, pp. 1–13, 2020, doi: 10.3390/molecules25051241.

[6] Y. Shen and I. Dierking, “Perspectives in liquid-crystal-aided nanotechnology and nanoscience,” *Appl. Sci.*, vol. 9, no. 12, 2019, doi: 10.3390/app9122512.

[7] D. Dunmur, “Liquid crystal chemistry and poetry,” *Found. Chem.*, vol. 23, no. 2, pp. 277–287, Jul. 2021, doi: 10.1007/s10698-020-09394-0.

[8] M. P. Allen, M. A. Warren, M. R. Wilson, A. Sauron, and W. Smith, “Liquid Crystals Liquid Crystals,” *Physics-Uspekhi*, vol. 2850, no. 4, pp. 551–573, 1996.

[9] H. Kawamoto, “The History of Liquid-Crystal Display and Its Industry.”

[10] M. Schadt, “Plenary lecture: The history of the liquid crystal display and

liquid crystal material technology," *Liq. Cryst.*, vol. 5, no. 1, pp. 57–71, 1989, doi: 10.1080/02678298908026352.

[11] H. Kelker, "Survey of the Early History of Liquid Crystals," *Mol. Cryst. Liq. Cryst. Inc. Nonlinear Opt.*, vol. 165, no. 1, pp. 1–43, Dec. 1988, doi: 10.1080/00268948808082195.

[12] H. Kelker, "HISTORY OF LIQUID CRYSTALS.," *Mol Cryst Liq Cryst*, vol. 21, no. 1–2, pp. 1–48, 1973, doi: 10.1080/15421407308083312.

[13] P. J. Collings, "Liquid Crystals: Fundamentals," *Phys. Today*, vol. 56, no. 11, pp. 69–70, 2003, doi: 10.1063/1.1634537.

[14] D. Dunmur, "Liquid crystal chemistry and poetry," *Found. Chem.*, vol. 23, no. 2, pp. 277–287, Jul. 2021, doi: 10.1007/s10698-020-09394-0.

[15] H.-G. Kuball, " From Chiral Molecules to Chiral Phases 1 : Comments on the Chirality of Liquid Crystalline Phases ," *Liq. Cryst. Today*, vol. 9, no. 1, pp. 1–7, May 1999, doi: 10.1080/13583149908047570.

[16] A. M. F. Neto and S. R. A. Salinas, "Phase Transitions and Structural Properties. The Physics of Lyotropic Liquid Crystals," pp. 5, 138, 2005.

[17] Athraa J. Ali and N. H. Karam, "Design of New V Shaped Thermotropic Liquid Crystals containing Heterocyclic," *Ibn AL-Haitham J. Pure Appl. Sci.*, vol. 36, no. 2, pp. 251–258, Apr. 2023, doi: 10.30526/36.2.3046.

[18] L. Zhang *et al.*, "Visible Light Responsive DNA Thermotropic Liquid Crystals Based on a Photothermal Effect of Gold Nanoparticles," *J. Anal. Test.*, vol. 5, no. 2, pp. 181–187, Jun. 2021, doi: 10.1007/s41664-020-00150-z.

[19] A. Carolina Sparavigna, "Role of Lyotropic Liquid Crystals in Templating Mesosilica Materials," *Int. J. Sci.*, vol. 12, no. 07, pp. 7–40, 2023, doi: 10.18483/ijsci.2691.

[20] M. Tarsitano, A. Mancuso, M. C. Cristiano, D. Paolino, and M. Fresta, "In Situ Swelling Formulation of Glycerol-Monooleate-Derived Lyotropic Liquid Crystals Proposed for Local Vaginal Application," *Molecules*, vol. 27, no. 19, Oct. 2022, doi: 10.3390/molecules27196295.

[21] A. Ryabchun, F. Lancia, J. Chen, D. Morozov, B. L. Feringa, and N. Katsonis, “Helix Inversion Controlled by Molecular Motors in Multistate Liquid Crystals,” *Adv. Mater.*, vol. 32, no. 47, Nov. 2020, doi: 10.1002/adma.202004420.

[22] C. D. Schimming and J. Viñals, “Computational molecular field theory for nematic liquid crystals,” *Phys. Rev. E*, vol. 101, no. 3, Feb. 2020, doi: 10.1103/PhysRevE.101.032702.

[23] M. Siavashpouri, C. H. Wachauf, M. J. Zakhary, F. Praetorius, H. Dietz, and Z. Dogic, “Molecular engineering of chiral colloidal liquid crystals using DNA origami,” *Nat. Mater.*, vol. 16, no. 8, pp. 849–856, Aug. 2017, doi: 10.1038/nmat4909.

[24] C. Li, Y. Liu, X. Huang, C. Li, and H. Jiang, “Light Actuation of Graphene-Oxide Incorporated Liquid Crystalline Elastomer Nanocomposites,” *Mol. Cryst. Liq. Cryst.*, vol. 616, no. 1, pp. 83–92, Jul. 2015, doi: 10.1080/15421406.2014.990256.

[25] A. A. Zaki, M. Hagar, R. B. Alnoman, M. Jaremko, A. H. Emwas, and H. A. Ahmed, “Mesomorphic, optical and dft aspects of near to room-temperature calamitic liquid crystal,” *Crystals*, vol. 10, no. 11, pp. 1–21, Nov. 2020, doi: 10.3390/cryst10111044.

[26] P. Salamon, N. Iber, Á. Buka, J. T. Gleeson, S. Sprunt, and A. Jákli, “Dielectric properties of mixtures of a bent-core and a calamitic liquid crystal,” *Phys. Rev. E - Stat. Nonlinear, Soft Matter Phys.*, vol. 81, no. 3, Mar. 2010, doi: 10.1103/PhysRevE.81.031711.

[27] I. Dierking, H. K. Chan, F. Culfaz, and S. McQuire, “Fractal growth of a conventional calamitic liquid crystal,” *Phys. Rev. E - Stat. Physics, Plasmas, Fluids, Relat. Interdiscip. Top.*, vol. 70, no. 5, p. 8, 2004, doi: 10.1103/PhysRevE.70.051701.

[28] G. Karanlik, H. Ocak, N. Y. Canli, M. Okutan, and B. B. Eran, “The dielectric parameters of a pyridine-based calamitic liquid crystal,” *Mater. Res. Express*, vol. 6, no. 11, Oct. 2019, doi: 10.1088/2053-1591/ab4be1.

[29] M. Munna, F. Anwar, and R. A. Coutu, “Nematic Liquid Crystal Composite

Materials for DC and RF Switching," *Technologies*, vol. 7, no. 2. MDPI, Jun. 01, 2019. doi: 10.3390/technologies7020032.

[30] D. Jiang, T. Huang, and Z. Shao, "Research of Nematic Liquid Crystal Broadband tunable power divider," in *2014 IEEE International Conference on Communication Problem-Solving, ICCP 2014*, 2014, pp. 517–519. doi: 10.1109/ICCPS.2014.7062337.

[31] I. Muševič, "Nematic liquid-crystal colloids," *Materials*, vol. 11, no. 1. MDPI AG, Dec. 25, 2017. doi: 10.3390/ma11010024.

[32] O. Parodi, L. J. De Physique, T. 31, and J. 1970, "Stress tensor for a nematic liquid crystal STRESS TENSOR FOR A NEMATIC LIQUID CRYSTAL Des équations constitutives pour les cristaux liquides nématiques ont été établies par Ericksen et Leslie. Dans ces équations apparait un tenseur des contraintes faisant," *J. Phys.*, no. 7, pp. 581–584, 1970, doi: 10.1051/jphys:01970003107058100ï.

[33] B. Zappone and E. Lacaze, "One-dimensional patterns and topological defects in smectic liquid crystal films," *Liquid Crystals Reviews*. pp. 1–18, 2022. doi: 10.1080/21680396.2022.2076748.

[34] M. E. Prévôt *et al.*, "Synchrotron microbeam diffraction studies on the alignment within 3d-printed smectic-a liquid crystal elastomer filaments during extrusion," *Crystals*, vol. 11, no. 5, 2021, doi: 10.3390/cryst11050523.

[35] M. P. Kumar, P. Kula, and S. Dhara, "Smecticlike rheology and pseudolayer compression elastic constant of a twist-bend nematic liquid crystal," *Phys. Rev. Mater.*, vol. 4, no. 11, Aug. 2020, doi: 10.1103/PhysRevMaterials.4.115601.

[36] S. Chandrasekhar and G. S. Ranganath, "Discotic liquid crystals," *Reports Prog. Phys.*, vol. 53, no. 1, pp. 57–84, 1990, doi: 10.1088/0034-4885/53/1/002.

[37] S. Chandrasekhar, "Discotic liquid crystals. A brief review," *Liq Cryst.*, vol. v. 14, no. March 2013, p. p.3-14, 1993, [Online]. Available: http://www.tandfonline.com/doi/abs/10.1080/02678299308027301

[38] S. Sergeyev, W. Pisula, and Y. H. Geerts, “Discotic liquid crystals: A new generation of organic semiconductors,” *Chem. Soc. Rev.*, vol. 36, no. 12, pp. 1902–1929, 2007, doi: 10.1039/b417320c.

[39] A. R. Hemsley and N. I. Gabarayeva, “Exine development: The importance of looking through a colloid chemistry ‘window,’” *Plant Syst. Evol.*, vol. 263, no. 1–2, pp. 25–49, 2007, doi: 10.1007/s00606-006-0465-2.

[40] M. M. Telo Da Gama, “Phase transitions in liquid crystal films,” *Phys. A Stat. Mech. its Appl.*, vol. 172, no. 1–2, pp. 219–224, 1991, doi: 10.1016/0378-4371(91)90322-4.

[41] I. Dierking, “Chiral liquid crystals: Structures, phases, effects,” *Symmetry (Basel).*, vol. 6, no. 2, pp. 444–472, 2014, doi: 10.3390/sym6020444.

[42] V. Palacio-Betancur, J. C. Armas-Pérez, J. P. Hernández-Ortiz, and J. J. de Pablo, “Curvature and confinement effects on chiral liquid crystal morphologies,” *Soft Matter*, vol. 19, no. 32, pp. 6066–6073, 2023, doi: 10.1039/d3sm00437f.

[43] S. Entanglement and S. It, “Physical Review Letters [2, 3, 4],” pp. 10–13, 2013.

[44] Amalia Yunia Rahmawati, “済無No Title No Title No Title,” vol. 25, no. July, pp. 1–23, 2020.

[45] G. Pelzl and A. Hauser, “Birefringence and phase transitions in liquid crystals,” *Phase Transitions*, vol. 37, no. 1, pp. 33–62, 1991, doi: 10.1080/01411599108203447.

[46] R. L. C. Vink, “Liquid crystals in two dimensions: First-order phase transitions and nonuniversal critical behavior,” *Phys. Rev. Lett.*, vol. 98, no. 21, pp. 1–4, 2007, doi: 10.1103/PhysRevLett.98.217801.

[47] H. H. Wensink and R. L. C. Vink, “Liquid crystals in two dimensions: First-order phase transitions and nonuniversal critical behavior,” *J. Phys. Condens. Matter*, vol. 19, no. 46, 2007, doi: 10.1103/PhysRevLett.98.217801.

[48] G. Jaeger, “The ehrenfest classification of phase transitions: Introduction and

evolution," *Arch. Hist. Exact Sci.*, vol. 53, no. 1, pp. 51–81, 1998, doi: 10.1007/s004070050021.

[49] T. Carlsson, "THEORETICAL INVESTIGATION OF THE SHEAR FLOW OF NEMATIC LIQUID CRYSTALS WITH THE LESLIE VISCOSITY alpha 3 greater than 0: HYDRODYNAMIC ANALOGUE OF FIRST ORDER PHASE TRANSITIONS.," *Mol. Cryst. Liq. Cryst.*, vol. 104, no. 3–4, pp. 307–334, 1984, doi: 10.1080/00268948408070434.

[50] J. Thoen, G. Cordoyiannis, and C. Glorieux, "Investigations of phase transitions in liquid crystals by means of adiabatic scanning calorimetry," *Liq. Cryst.*, vol. 36, no. 6–7, pp. 669–684, 2009, doi: 10.1080/02678290902755564.

[51] A. N. Zakhlevnykh and O. R. Semenova, "First order orientational transitions in ferronematic liquid crystals," in *Molecular Crystals and Liquid Crystals*, 2011, pp. 219–226. doi: 10.1080/15421406.2011.568887.

[52] P. Molignini, *Analyzing the two dimensional Ising model with conformal field theory*, no. May. 2013.

[53] N. Y. CANLI, "INVESTIGATION OF MESOMORPHIC, MORPHOLOGICAL AND ELECTRO-OPTICAL PROPERTIES OF LIQUID CRYSTAL SYSTEMS," 2008.

[54] A. Majumdar and A. Zarnescu, "Landau-De Gennes theory of nematic liquid crystals: The Oseen-Frank limit and beyond," *Arch. Ration. Mech. Anal.*, vol. 196, no. 1, pp. 227–280, 2010, doi: 10.1007/s00205-009-0249-2.

[55] A. Majumdar and A. Zarnescu, "Crystals : the Oseen – Frank Limit and Beyond," vol. 196, pp. 227–280, 2010.

[56] I. C. Gârlea and B. M. Mulder, "The Landau-de Gennes approach revisited: A minimal self-consistent microscopic theory for spatially inhomogeneous nematic liquid crystals," *J. Chem. Phys.*, vol. 147, no. 24, 2017, doi: 10.1063/1.4993574.

[57] J. F. C. Turner and B. Hall, "Gibbs free energy," *Encycl. Earth Sci. Ser.*, vol. Part 4, p. 323, 2011, doi: 10.1007/978-1-4419-6247-8_5492.

[58] G. Arzpeyma, A. E. Gheribi, and M. Medraj, "On the prediction of Gibbs

free energy of mixing of binary liquid alloys," *J. Chem. Thermodyn.*, vol. 57, pp. 82–91, 2013, doi: 10.1016/j.jct.2012.07.020.

[59] G. ÖNSAL, "INVESTIGATION OF DIELECTRIC PROPERTIES OF MBBA-5CB NEMATIC LIQUID CRYSTAL STRUCTURES," *Mugla J. Sci. Technol.*, vol. 8, no. 2, pp. 49–53, Dec. 2022, doi: 10.22531/muglajsci.1198432.

[60] P. Kopčanský *et al.*, "Dielectric properties of lyotropic magnetic liquid crystal," in *Acta Physica Polonica A*, Polska Akademia Nauk, Feb. 2015, pp. 632–634. doi: 10.12693/APhysPolA.127.632.

[61] R. Mao *et al.*, "Dielectric Properties of Liquid Crystal Polymer Substrates in the Region from 90 to 140 GHz," *Crystals*, vol. 12, no. 2, Feb. 2022, doi: 10.3390/cryst12020170.

[62] T. Pícha and S. Papežová, "Dielectric properties of materials for 3D printing at high frequencies," *Res. Agric. Eng.*, vol. 69, no. 1, pp. 28–35, 2023, doi: 10.17221/10/2022-RAE.

[63] S. S. Zhekov, O. Franek, and G. F. Pedersen, "Dielectric Properties of Common Building Materials for Ultrawideband Propagation Studies [Measurements Corner]," *IEEE Antennas Propag. Mag.*, vol. 62, no. 1, pp. 72–81, Feb. 2020, doi: 10.1109/MAP.2019.2955680.

[64] S. A. Rosales, F. González, F. Moreno, and Y. Gutiérrez, "Non-absorbing dielectric materials for surface-enhanced spectroscopies and chiral sensing in the UV," *Nanomaterials*, vol. 10, no. 10, pp. 1–22, Oct. 2020, doi: 10.3390/nano10102078.

[65] W. Otowski and G. Lewińska, "Dielectric properties and molecular motions of liquid crystal molecules in 4-(2-methylbytyl)phenyl 4-(4-octylphenyl)benzoate liquid crystal having blue phase (CE8)," *Mater. Sci. Pol.*, vol. 33, no. 2, pp. 418–429, 2015, doi: 10.1515/msp-2015-0044.

[66] M. Škarabot *et al.*, "Flexoelectric Polarization in a Nematic Liquid Crystal Enhanced by Dopants with Different Molecular Shape Polarities," *ACS Omega*, vol. 7, no. 11, pp. 9785–9795, Mar. 2022, doi: 10.1021/acsomega.2c00023.

[67] I. Zachmann, A. Svanidze, Q. Zhang, L. Ji, K. Johnson, and C. Mao, "Development of thin film quarter-waveplate for polarization-independent liquid crystal on silicon phase modulators," *Opt. Eng.*, vol. 62, no. 06, Jun. 2023, doi: 10.1117/1.oe.62.6.065105.

[68] Y. Yuan, C. Yao, W. Shen, X. Hu, and C. Hu, "Polarization Measurement Method Based on Liquid Crystal Variable Retarder (LCVR) for Atomic Thin-Film Thickness," *Nanomanufacturing Metrol.*, vol. 5, no. 2, pp. 159–166, Jun. 2022, doi: 10.1007/s41871-022-00131-z.

[69] T. Le, H. Tran, B. Pejcinovic, K. G. R. Thompson, R. Doneker, and A. Ramachandran, "Development and Characterization of Carbon-Fiber Based Magnetically Loaded Microwave Absorber Material," in *IEEE International Symposium on Electromagnetic Compatibility*, 2018, pp. 767–771. doi: 10.1109/EMCEurope.2018.8485065.

[70] P.-C. Wu, C.-T. Hou, Y.-C. Hsiao, and W. Lee, "Influence of methyl red as a dopant on the electrical properties and device performance of liquid crystals," *Opt. Express*, vol. 22, no. 25, p. 31347, Dec. 2014, doi: 10.1364/oe.22.031347.

[71] I. Pasternak, R. Pasternak, and H. Sulym, "Temperature field and heat flux that do not induce stress and electric displacement in a free thermoelectroelastic anisotropic solid," *Mech. Res. Commun.*, vol. 57, pp. 40–43, 2014, doi: 10.1016/j.mechrescom.2014.02.004.

[72] C. Linder and C. Miehe, "Effect of electric displacement saturation on the hysteretic behavior of ferroelectric ceramics and the initiation and propagation of cracks in piezoelectric ceramics," *J. Mech. Phys. Solids*, vol. 60, no. 5, pp. 882–903, May 2012, doi: 10.1016/j.jmps.2012.01.012.

[73] O. M. Y and I. J. T, "Frequency and Temperature Dependence of Ethanol Using the Cole-Cole Relaxation Model," *Am. J. Condens. Matter Phys.*, vol. 2020, no. 2, pp. 44–49, doi: 10.5923/j.ajcmp.20201002.03.

[74] M. Sahraoui, A. Abderrahmen, R. Mlika, H. Ben Ouada, and A. Gharbi, "Dielectric relaxation behavior of nematic liquid crystal cell using β-cyclodextrin as an alignment layer," *Mediterr. J. Chem.*, vol. 5, no. 1, pp. 347–355, Feb. 2016, doi: 10.13171/mjc.5.1/0160209/sahraoui.

[75] S. Holm, “Time domain characterization of the Cole-Cole dielectric model,” *J. Electr. Bioimpedance*, vol. 11, no. 1, pp. 101–105, 2020, doi: 10.2478/JOEB-2020-0015.

[76] C. Huang and L. L. Wang, “An accurate spectral method for the transverse magnetic mode of Maxwell equations in Cole-Cole dispersive media,” *Adv. Comput. Math.*, vol. 45, no. 2, pp. 707–734, 2019, doi: 10.1007/s10444-018-9636-2.

[77] T. Budtova and P. Navard, “Viscosity-temperature dependence and activation energy of cellulose solutions,” *Nord. Pulp Pap. Res. J.*, vol. 30, no. 1, pp. 99–104, 2015, doi: 10.3183/npprj-2015-30-01-p099-104.

[78] R. M. Rubinger *et al.*, “Temperature-dependent activation energy and variable range hopping in semi-insulating GaAs,” *Semicond. Sci. Technol.*, vol. 21, no. 12, pp. 1681–1685, 2006, doi: 10.1088/0268-1242/21/12/030.

[79] B. Suryanto, D. Saraireh, and A. Tambusay, “Temperature dependence and activation energy of electrical conduction in an engineered cementitious composite,” *IOP Conf. Ser. Mater. Sci. Eng.*, vol. 930, no. 1, 2020, doi: 10.1088/1757-899X/930/1/012053.

[80] J. V. Li, S. W. Johnston, Y. Yan, and D. H. Levi, “Measuring temperature-dependent activation energy in thermally activated processes: A 2D Arrhenius plot method,” *Rev. Sci. Instrum.*, vol. 81, no. 3, 2010, doi: 10.1063/1.3361130.

[81] W. Sima, “4-[(2′-Cyanobiphenyl-4-yl)methyl]-morpholin-4-ium nitrate,” *Acta Crystallogr. Sect. E Struct. Reports Online*, vol. 66, no. 8, Aug. 2010, doi: 10.1107/S1600536810027443.

[82] T. Koda *et al.*, “Effect of charge transfer complex on electrical properties of 4-cyano-4′-pentylbiphenyl,” *Jpn. J. Appl. Phys.*, vol. 48, no. 12, Dec. 2009, doi: 10.1143/JJAP.48.121404.

[83] H. Y. Ou-Yang, “4-[(2′-Cyano-biphenyl-4-yl)meth-yl]morpholin-4-ium perchlorate,” *Acta Crystallogr. Sect. E Struct. Reports Online*, vol. 68, no. 4, Apr. 2012, doi: 10.1107/S1600536812012792.

[84] D. Agranovich, E. Polygalov, I. Popov, P. Ben Ishai, and Y. Feldman,

"Inductive dielectric analyzer," *Meas. Sci. Technol.*, vol. 28, no. 3, Jan. 2017, doi: 10.1088/1361-6501/aa56a7.

[85] P. Jagadeesh, G. K. K. Reddy, and S. V. Reddy, "Design and Development of an Inexpensive Temperature Controller for an Infant Incubator," *Int. J. Adv. Res. Electr. Electron. Instrum. Energy*, vol. 3, pp. 10194–10201, 2014, [Online]. Available: www.ijareeie.com

[86] M. Z. Wahyudi, D. W. Pratama, A. Fitrian, M. Abdillah, and H. Setiadi, "Temperature Control using PI Controller," *J. Emerg. Supply Chain. Clean Energy, Process Eng.*, vol. 1, no. 1, pp. 75–83, Sep. 2022, doi: 10.57102/jescee.v1i1.8.

[87] X. For and O. M. Battaini, "B -s e s c," pp. 1–20, 1998.

[88] M. Naylor and S. Moore, "A generic synthesisable test bench," in *2015 ACM/IEEE International Conference on Formal Methods and Models for Codesign, MEMOCODE 2015*, 2015, pp. 128–137. doi: 10.1109/MEMCOD.2015.7340479.

[89] E. R. Rwenyagila, I. N. Makundi, N. R. Mlyuka, and M. E. Samiji, "Dielectric anomalous peaks accenting ferroelectricity prospects of Li and Mg co-doped ZnO ceramics," *Results Mater.*, vol. 12, Dec. 2021, doi: 10.1016/j.rinma.2021.100226.

PUBLICATIONS FROM THE THESIS

Conference Papers

1. Paper 1

IHAB SALAH MAHDI attended 9th International Materials Science and Nanotechnology for Next Generation Conference held in Gazi University, Ankara, Türkiye Titled "Comparison of Dielectric Properties of 1wt.% SmC* LC Doped Nematic LC" at 23 September 2022.